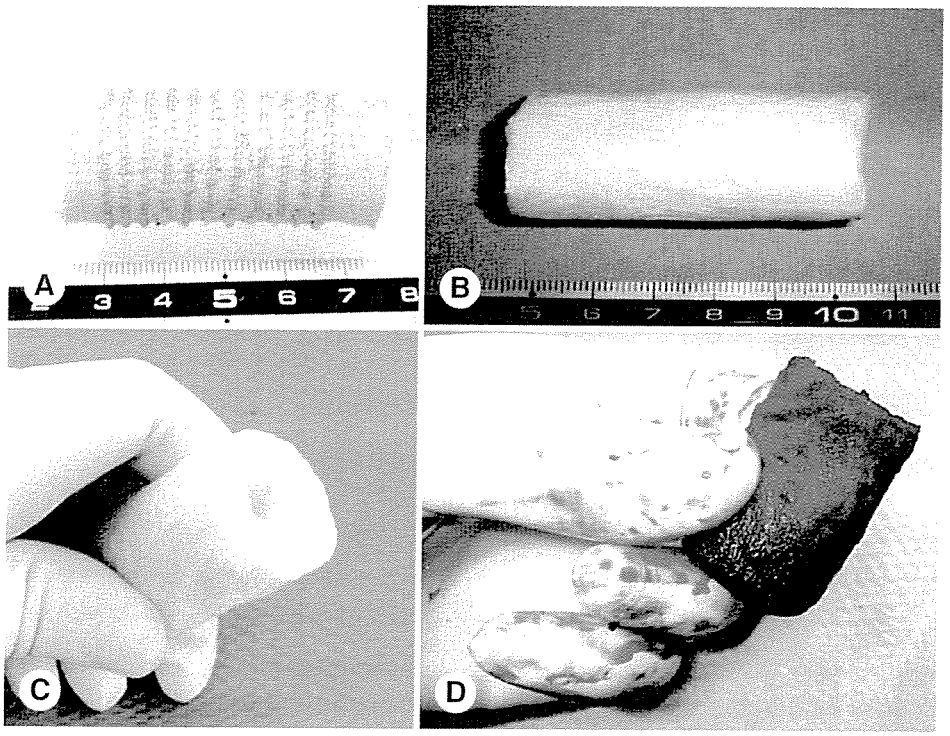


**Fig 2.** Artificial material. **A)** Marlex mesh tube with spiral ring. **B)** Marlex mesh tube with spiral ring coated with collagen sponge. **C)** Artificial material trimmed to size of defect. **D)** Injection of autologous blood into collagen sponge.

neering technology consists of three factors: scaffold, cells, and regulation factors, as shown in Fig 1. Depending on the situation at the site of application, these elements are chosen and applied in combination. On the basis of the novel concept of in situ tissue engineering, in contrast to ex vivo tissue engineering, our group has developed a collagen sponge scaffold to support tissue regeneration and has used it successfully to repair defects in the trachea, esophagus, stomach, and intestine in animal models.[4-7,9-11] The collagen sponge scaffold provides favorable conditions for tissue regeneration in vivo in combination with infiltrated host cells and regulation factors released from the surrounding tissue.

Previously, for the experimental studies of an animal model for airway regeneration, 32 beagle dogs were used for operation under general anesthesia. The animal care, housing, and surgery followed the Guidelines of the Animal Experiment Committee, Kyoto University (1983).

In 24 of the 32 dogs, a 45-mm segment of the tra-

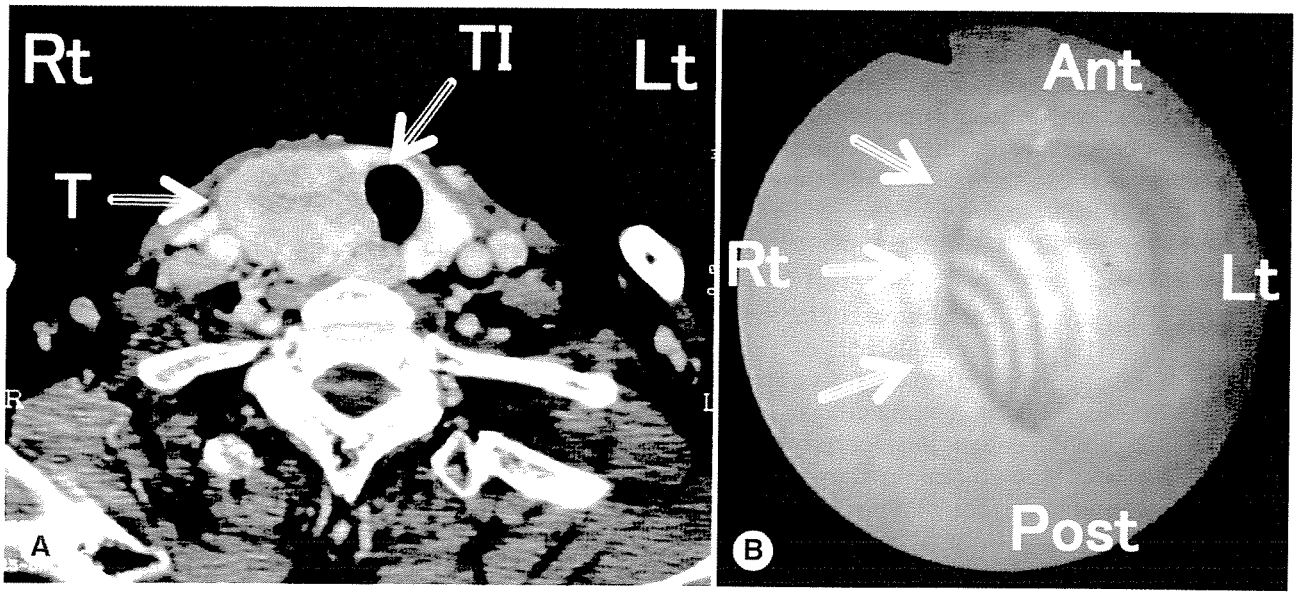


**Fig 3.** Preoperative investigation. **A)** Computed tomography scan. T — tumor, TI — tracheal invasion. **B)** Endoscopic findings. Arrows indicate tumor invasion into trachea.

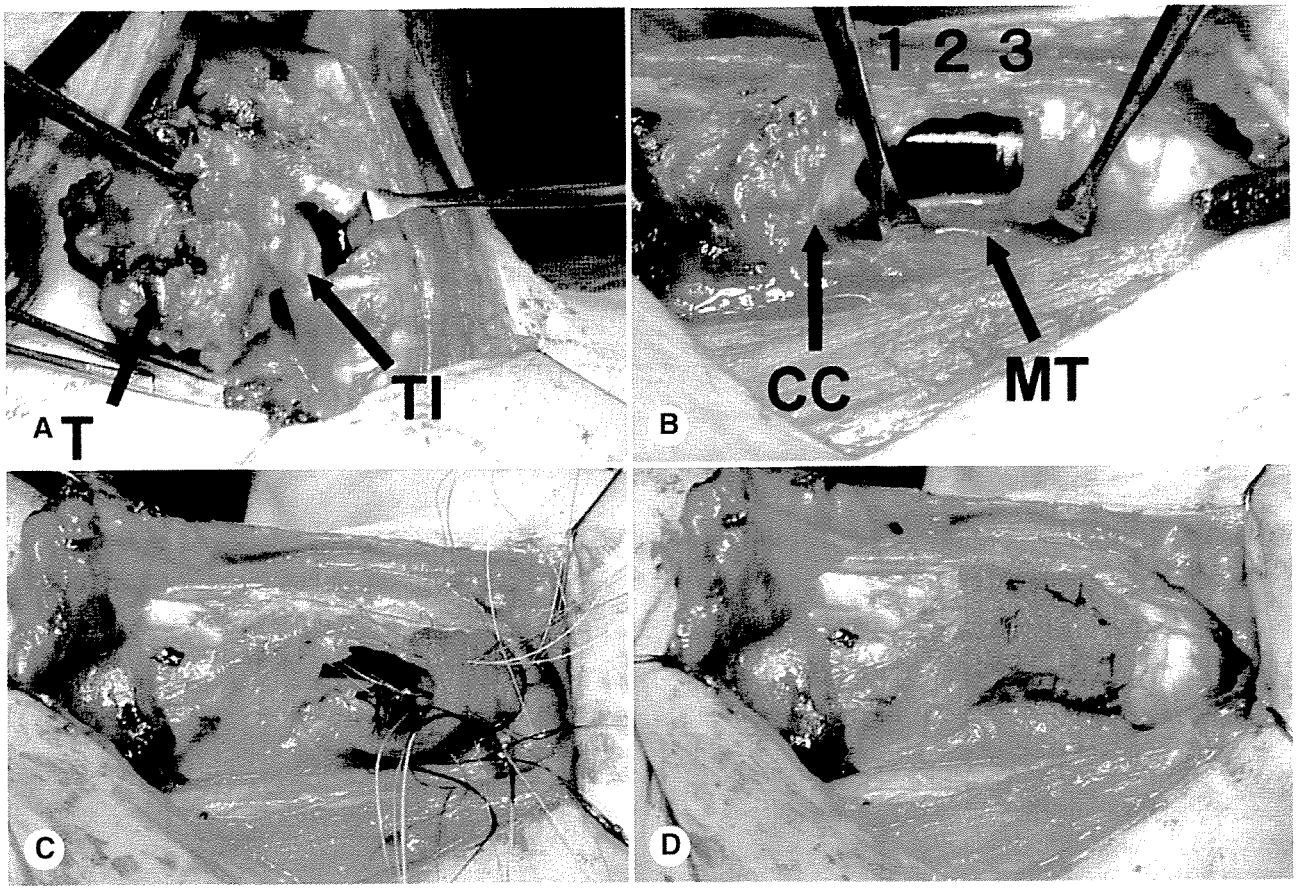


**Fig 4.** Operative procedures. **A)** Invasion of tracheal cartilage by tumor (T) of right lobe of thyroid gland. TI — tracheal invasion. **B)** Resected tracheal cartilage. CC — cricoid cartilage, MT — membranous trachea, 1 — first tracheal ring, 2 — second tracheal ring, 3 — third tracheal ring. **C)** Suturing of artificial material to defect. **D)** After implantation of artificial material.

chea was resected circumferentially 30 mm from the carina, and the Marlex mesh tube with collagen sponge was implanted as a scaffold material.[6] Postoperative endoscopy for a period of 3 to 60 months showed a well-epithelialized tracheal lumen without airway obstruction.[7] Light microscopy showed that the Marlex mesh was completely incorporated within the connective tissue. Scanning electron microscopy showed regeneration of the cilial epithelium. Mechanical tests showed that the stress-strain curve of the regenerated tissue was similar to that of the normal tracheal cartilage, demonstrating a firmly supported airway framework.

In 8 of the 32 dogs, the anterior part of the cricoid cartilage and/or the cartilaginous part of rings 1 through 5 of the trachea were resected. As a scaffold material, a Marlex mesh tube with collagen sponge was implanted into the defect. Postoperative endoscopy for a period of 3 to 26 months showed a well-epithelialized luminal surface with no airway stenosis in any of the 8 dogs. Although granulation was observed in 2 cases and a small part of the Marlex mesh was exposed in 1 case, these dogs were asymptomatic in terms of respiration.[12]

On the basis of the previous experimental studies of tracheal tissue regeneration using an in situ tissue engineering technique in animal models, this regenerative technique was applied for repair of the tracheal defect in a human case of tracheal invasion from thyroid cancer.

## SCAFFOLD MATERIAL

An artificial material — a Marlex mesh tube covered by collagen sponge — was used for the tissue scaffold. An approximately 50-mm-long Marlex mesh tube with an outer diameter of 15 mm was made from polypropylene mesh with a pore size of 260 μm (CR Bard Inc, Billerica, Massachusetts) and implanted in a human case as presented below (Fig 2A). This tube was reinforced with a polypropylene spiral ring. The inner and outer sides of the Marlex mesh tube were coated with collagen sponge made from porcine dermal atelocollagen (Nippon Meatpackers Inc, Ibaraki, Japan) consisting of type 1 and type 3 collagen dissolved in hydrochloric acid solution, pH 3.0, at a concentration of 1.0% (Fig 2B). The artificial tube was corona-discharged at 9 kV to activate the polymer surface in order to immobilize the colla-

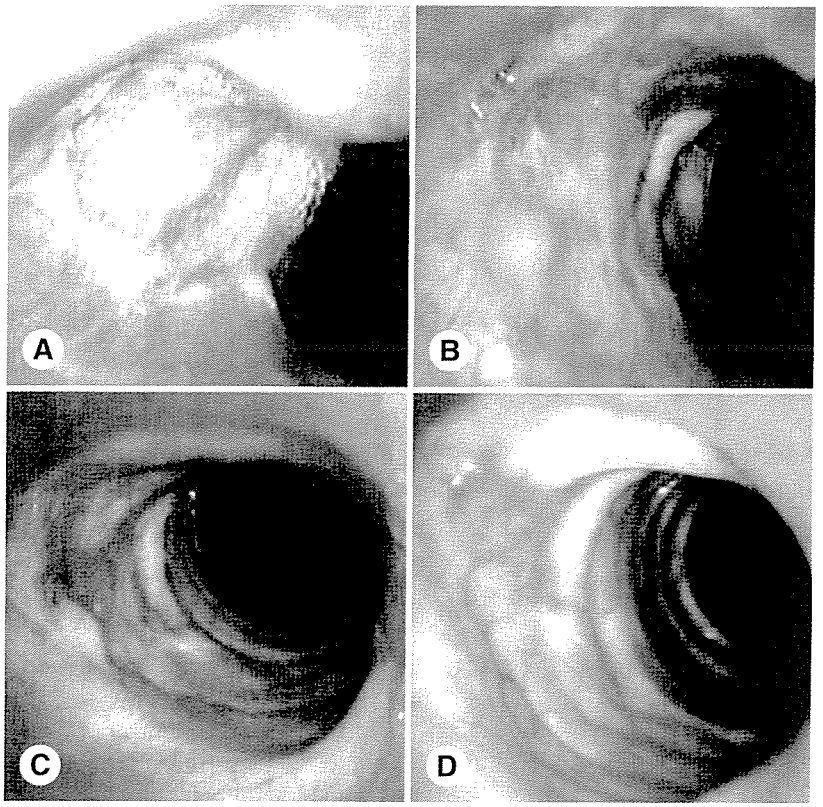


**Fig 5.** Endoscopic findings. **A)** After 2 weeks. **B)** After 2 months. **C)** After 7 months. **D)** After 20 months.

gen molecules and was heated at 140°C in vacuo in order to induce cross-linking between the collagen molecules.

## CASE REPORT

This newly developed method for regeneration of the tracheal tissue was applied to a human patient for evaluation of its practical use in accordance with the guidelines of the Ethics Committee, Kyoto University Graduate School and Faculty of Medicine. A 78-year-old woman had swelling in the right side of her neck. A computed tomography scan showed heterogeneous tumor involving the right lobe of the thyroid gland, as shown in Fig 3A. Fine-needle aspiration biopsy of the tumor revealed papillary adenocarcinoma, class V. Preoperative testing showed a thyroid-stimulating hormone level of 8.9 μU/mL, a free tetraiodothyroxine level of 1.12 ng/dL, a free triiodothyroxine level of 3.74 pg/mL, and a thyroglobulin level of 423 ng/mL. Endoscopic examination showed bulging of the right luminal surface of the trachea, just below the subglottis (Fig 3B). This finding indicated tumor invasion into the tracheal tissue.

With informed consent, the patient underwent the current regenerative treatment of the tracheal tissue using the artificial material in 2002. Under general anesthesia, the operative intervention included right hemithyroidectomy, resection of the trachea, and tracheoplasty using the artificial material, Marlex mesh with collagen sponge. The artificial material was trimmed (Fig 2C), and autologous venous blood was injected into the collagen for air-tightness, watertightness, and release of endogenous factors (Fig 2D). The tumor had invaded the second ring of the tracheal cartilage on the right side (Fig 4A). The right half of three rings of the trachea was resected (Fig 4B). The material was sutured to the edge of the trachea with 4-0 Vicryl absorbable thread (Fig 4C,D). When the anesthesia had worn off, the endotracheal tube was removed in the operating room. After 2 weeks, the mesh collagen structure of the artificial material could be seen with endoscopy in most of the implanted area (Fig 5A). The artificial material was covered with epithelial growth after 2 months (Fig 5B). Good epithelialization was shown on most of the artificial material after 7 months (Fig 5C). Epithelial growth had covered the artificial material completely by 20 months with no complications (Fig 5D), and further observation approximately 5 months later supported this conclusion.

## DISCUSSION

Reconstruction of the larynx and trachea in cases of malignancies or stenotic lesions is one of the most difficult surgical treatments. Bone graft, cartilage graft, muscle graft, and skin graft, among other techniques, have been used for repair of the airway defect.[1,2] These techniques following laryngeal and/or

tracheal resection required several complicated procedures for reconstructing both the airway framework and the luminal surface.

Artificial tracheal prostheses have been developed; however, almost all of the trials have ended unsuccessfully. Although the prosthesis of Neville et al,[3] which was made of silicone rubber with terminal Dacron suture rings, was once used clinically, dehiscence occurred at the interface between the prosthesis and the host tissue. Our group developed porous tracheal prostheses made of Marlex mesh with collagen sponge, which were designed for inducing tissue invasion into the material.[4-7] Collagen sponge provides not only air sealing but also enhancement of tissue invasion into the material. A Y-shaped tracheal prosthesis was implanted, and tracheal tissue was successfully regenerated in animal experiments, as well as with a straight-type tracheal prosthesis.

Tissue engineering technology consists of three factors: scaffold, cells, and regulation factors.[8] Highly differentiated tissues and organs are able to regenerate under the appropriate conditions. In situ tissue engineering of the trachea, esophagus, stomach, and intestine has been studied by implantation of collagen sponge as a scaffold graft without additional cells or outside regulation factors.[4-7,9-11] According to the results, the collagen sponge scaffold could provide favorable conditions for tissue regeneration in vivo in combination with infiltrated host cells and regulation factors released during the inflammatory process. It has been reported that collagen, which is a component of the extracellular matrix, induces cell transformation, division, proliferation, and detachment.[13] During repair of injured tissues and organs, endogenous factors are naturally secreted at damaged sites as regulation factors.[14]

In our experimental studies, histologic findings showed good incorporation of the scaffold mesh into the host tissue and regeneration of the ciliated epithelium over the mesh tube. Mechanical tests demonstrated that the regenerated tissue firmly supported the airway framework for respiration. The Marlex mesh tube with collagen provided a good environment for regenerating the subglottic and tracheal epithelium without the addition of cells or outside regulation factors.

On the basis of successful experimental studies, this newly developed method for regeneration of the tracheal tissue was applied to a human patient. In this case, the right half of three rings of the trachea was resected. The defect was not too large for use of the conventional techniques; however, the current regenerative technique avoided tracheotomy, a second operation, and deformity. Good epithelialization has been observed on the tracheal luminal surface without any complications for 2 years (as of January 2005). Although long-term follow-up is required, in situ tissue engineering of the tracheal tissue is feasible and practical after resection of the trachea with airway lesions of malignancies or stenosis.

## REFERENCES

1. Cotton RT. Management of subglottic stenosis. Otolaryngol Clin North Am 2000;33:111-30.

2. Caputo V, Consiglio V. The use of patient's own auricular cartilage to repair deficiency of the tracheal wall. J Thorac Cardiovasc Surg 1961;41:594-6.

3. Neville WE, Bolanowski PJ, Kotia GG. Clinical experience with the silicone tracheal prosthesis. J Thorac Cardiovasc Surg 1990;99:604-13.

4. Teramachi M, Kiyotani T, Takimoto Y, Nakamura T, Shimizu Y. A new porous tracheal prosthesis sealed with collagen sponge. ASAIO J 1995;41:M306-M310.

5. Teramachi M, Nakamura T, Yamamoto Y, Kiyotani T, Takimoto Y, Shimizu Y. Porous-type tracheal prosthesis sealed with collagen sponge. Ann Thorac Surg 1997;64:965-9.

6. Teramachi M, Okumura N, Nakamura T, et al. Intrathoracic tracheal reconstruction with a collagen-conjugated prosthesis: evaluation of the efficacy of omental wrapping. J Thorac Cardiovasc Surg 1997;113:701-11.

7. Nakamura T, Teramachi M, Sekine T, et al. Artificial trachea and long term follow-up in carinal reconstruction in dogs. Int J Artif Organs 2000;23:718-24.

8. Bianco P, Robey PG. Stem cells in tissue engineering. Nature 2001;414:118-21.

9. Yamamoto Y, Nakamura T, Shimizu Y, et al. Intrathoracic esophageal replacement in the dog with the use of an artificial esophagus composed of a collagen sponge with a double-layered silicone tube. J Thorac Cardiovasc Surg 1999;118:276-86.

10. Hori Y, Nakamura T, Matsumoto K, Kurokawa Y, Satomi S, Shimizu Y. Experimental study on in situ tissue engineering of the stomach by an acellular collagen sponge scaffold graft. ASAIO J 2001;47:206-10.

11. Hori Y, Nakamura T, Matsumoto K, Kurokawa Y, Satomi S, Shimizu Y. Tissue engineering of the small intestine by acellular collagen sponge scaffold grafting. Int J Artif Organs 2001; 24:50-4.

12. Omori K, Nakamura T, Kanemaru S, et al. Cricoid regeneration using in situ tissue engineering in canine larynx for the treatment of subglottic stenosis. Ann Otol Rhinol Laryngol 2004; 113:623-7.

13. Breuing K, Andree C, Helo G, Slama J, Liu PY, Eriksson E. Growth factors in the repair of partial thickness porcine skin wounds. Plast Reconstr Surg 1997;100:657-64.

14. Ruoslahti E, Hayman EG, Pierschbacher MD. Extracellular matrices and cell adhesion. Arteriosclerosis 1985;5:581-94.

# Fibroblast Growth Factor-2 Induces Recovery of Pulmonary Blood Flow in Canine Emphysema Models*

*Shigeyuki Morino, MD; Tatsuo Nakamura, MD; Toshinari Toba, MD; Mitsuru Takahashi, MD; Toshihiro Kushibiki, MD; Yasuhiko Tabata, MD; and Yasuhiko Shimizu, MD*

***Study objectives:*** **Fibroblast growth factor (FGF)-2 is one of the most powerful angiogenic growth factors to be evaluated as an agent for the promotion of angiogenesis. The aim of this study is to investigate whether intratracheal administration of controlled-release FGF-2 microspheres restores pulmonary function in beagle dogs with emphysema.**
***Design:*** **Randomized, controlled, experimental animal study.**
***Subjects:*** **Eighteen Wister rats and 15 adult beagle dogs.**
***Methods:*** **In the rat study, we compared the time profiles of the radioactivity remaining after intratracheal injection of $^{125}$I-labeled FGF-2, either incorporated with the controlled-release microspheres or as an aqueous solution. In the dog study, elastase-induced emphysema models were developed in 10 animals, classified into the following three groups: control group (n = 5), emphysema model with empty microspheres-treated group (FGF − group, n = 5), and emphysema model with FGF-2 containing microspheres-treated group (FGF + group, n = 5).**
***Results:*** **In the rat study, controlled-release microspheres maintained higher whole-lung FGF-2 concentrations after intratracheal administration. In the dog study, $Pao_2$ in the FGF + group was significantly higher than in the FGF − group after treatment. Pulmonary perfusion dynamic MRI revealed significant improvement in the signal intensity of damaged lung with the FGF + group. Linear intercept of the FGF + group was significantly reduced than the FGF − group.**
***Conclusion:*** **Results indicate that intratracheal administration of FGF-2 induced an increase in pulmonary blood flow in the damaged lung and led to recovery of pulmonary function. The controlled-release microsphere system increased the effectiveness of FGF-2.**
***(CHEST 2005; 128:920–926)***

**Key words:** angiogenesis; COPD; emphysema; fibroblast growth factor; regeneration

**Abbreviations:** FGF = fibroblast growth factor; FGF − group = emphysema model with empty microspheres-treated group; FGF + group = emphysema model with FGF-2 containing microspheres-treated group; Lm = mean linear intercept; P/V = pressure/volume; LVRS = lung volume reduction surgery

Lung volume reduction surgery (LVRS) improves lung function, exercise capacity, and quality of life in patients with advanced emphysema by allowing the remaining pulmonary parenchyma and the respiratory muscles to function more effectively. Although the physiologic and symptomatic benefits of LVRS have, on average, been impressive, the substantial rates of morbidity and mortality associated with major thoracic surgery and general anesthesia in an elderly, debilitated population have limited the clinical utility of the procedure. Moreover, patients with the most advanced disease have higher surgical mortality, suggesting that LVRS is not suitable for those with severe disease.[1,2] There is currently no therapy for the treatment of lung emphysema. Noninvasive treatment is desirable for severe emphysema patients.

Fibroblast growth factor (FGF)-2 is one of the most powerful angiogenic growth factors to be evaluated as an agent for the promotion of angiogenesis. Patients with severe emphysema have higher-than-normal pulmonary arterial pressure. Severe emphy-

*From the Institute for Frontier Medical Sciences (Drs. Nakamura, Toba, Takahashi, Kushibiki, Tabata, and Shimizu), Kyoto University, Kyoto; and Division of Surgical Oncology (Dr. Morino), Nagasaki University School of Medicine, Nagasaki, Japan.
FGF-2 was provided by Kaken Pharmaceutical Company, Tokyo, Japan; and gadopentetate dimeglumine was provided by Magnevist, Nihon Schering, Osaka, Japan.
Manuscript received September 2, 2004; revision accepted January 3, 2005.

*Correspondence to: Shigeyuki Morino, MD, Department of Bioartificial Organs, Institute for Frontier Medical Sciences, Kyoto University, 53 Kawaharacho, Shogoin, Sakyo-ku, Kyoto 606-8507, Japan; e-mail: morinos@frontier.kyoto-u.ac.jp*

sema also tends to produce diffuse microvessel abnormalities in the pulmonary peripheral arteries.[3] Induction of a collateral pulmonary vessel network is a potent method of providing effective relief from dyspnea, general fatigue, and other symptoms in emphysema. Polymer hydrogels composed of gelatin have previously been demonstrated to be suitable matrices for the controlled release of growth factors because of their biosafety and the fact that they are highly inert toward protein drugs.[4] Biodegradable gelatin microspheres incorporating FGF-2 have been developed using acidic gelatin hydrogels. The use of these microspheres enables FGF-2 to be released at the site of action over a sufficiently long period of time to act effectively, in remarkable contrast to free FGF-2.[5] The aim of the present study was to investigate whether there is a benefit of bronchoscopic administration of FGF-2 on elastase-induced emphysema animals.

## Materials and Methods

### *Distribution of FGF-2 Intratracheal Administration in Rats*

Eighteen female Wister rats weighing 250 to 300 g and 15 adult beagle dogs weighing 10.0 to 14.9 kg were used in this study. The study protocol was approved by the Kyoto University Ethics Committee for Animal Research. All animals received humane care in compliance with the Principles of Laboratory Animal Care formulated by the National Society for Medical Research and the Guide for the Care and Use of Laboratory Animals prepared by the Institute of Laboratory Animal Resources, National Research Council, and published by the National Academy Press.

The rats were anesthetized with pentobarbital sodium, and the trachea was exposed. All the FGF-2 was labeled by $^{125}I$. $^{125}I$-labeled FGF-2 was injected via 0.3 mL of solution to the trachea (FGF solution group, n = 9). $^{125}I$-labeled–FGF-2 microspheres were injected in 0.3 mL of suspended solution to the trachea (FGF microsphere group, n = 9). Lung tissues were obtained at different time intervals: 24 h, 72 h, and 7 days. The radioactivity remaining was calculated from the whole lung on a gamma counter (ARC-301B; Aloka; Tokyo, Japan).

### *Preparation of the Elastase-Induced Emphysema Model*

The 15 beagle dogs were classified at random into the following three groups: control group, emphysema model with empty microspheres-treated group (FGF − group), and emphysema model with FGF-2 containing microspheres-treated group (FGF +) group. Models of elastase-induced emphysema were developed in the FGF − and FGF + groups. All interventions and physiologic measurements were performed under general anesthesia with ketamine hydrochloride (10 mg/kg) and xylazine (30 mg/kg), and mechanical ventilation was administered through an endotracheal tube. A 9.0-mm diameter endotracheal tube was inserted into the trachea under bronchoscopic guidance and attached to a mechanical ventilator. Continuous monitoring included ECG, oxygen saturation by reflectance oximetry using a sensor clipped to the ear, and body temperature by means of a rectal probe. A bronchoscope (5 mm outside diameter and 60 cm working length) was introduced through the indwelling endotracheal tube and advanced to the left segmental bronchus. Then, 40 mg (3,000 U) of porcine pancreatic elastase (Nakarai Tesque; Kyoto, Japan) was dissolved in 5 mL of saline solution and sprayed into all segmental bronchi of the left lung through the instrument channel of the bronchoscope using a spray infusion catheter (Olympus Optical; Tokyo, Japan) in the elastase-induced emphysema models. Each elastase dose was divided into 10 portions, each of which was sprayed in a different area to make a model of diffuse emphysema at the level of the left segmental bronchus. The right lung was preserved intact as a control.

### *Arterial Blood Gas and Pressure/Volume Relationships*

Assessment of pulmonary function and MRI were performed before elastase administration (baseline), 4 weeks after elastase administration, and 4 weeks after treatment. For assessment of pulmonary function, dogs were anesthetized, intubated, and maintained on < 3.0% halothane. Arterial blood pH, $Paco_2$, $Pao_2$, and percentage of oxygen saturation were measured. Mechanical ventilation was set at a breathing frequency of 10 breaths/min, the inspiratory time was set to 33% of the breathing period, and the fraction of inspired oxygen was 0.2. Tidal volume was set to 18 mL/kg. Arterial blood gas samples were obtained from the right femoral artery 15 min after mechanical ventilation was started. A blood gas and acid-base analyzer (ABL-620; Radiometer; Copenhagen, Denmark) was used for measurements. Pressure/volume (P/V) relationships and expiratory capacity were also measured under general anesthesia with intubation. The intratracheal cavity was inflated to various pressures (5 to 70 cm $H_2O$), and the endotracheal tube was then clamped tightly. A plethysmograph (HI-701; Nihon Kohden; Tokyo, Japan) was connected to the endotracheal tube and the clamp was released, and then the expiratory capacity was measured. The expiratory capacity when the intratracheal cavity was inflated to a pressure of 40 cm $H_2O$ (expiratory capacity, 40 cm $H_2O$) was used for calculations.

### *Dynamic Contrast-Enhanced MRI*

All MRI studies were performed (1.5 T Sonata; Siemens Medical Systems; Erlangen, Germany) with a maximum amplitude of 40 mT/m and a rise time of 0.6 ms, using a phased-array body coil with four active segments. A turbo fast low-angle shot sequence optimized for projection imaging was used for dynamic contrast-enhanced MRI.[6] The following image parameters were used: echo time/repetition time, 1.35/350 ms; flip angle, 8°; readout bandwidth, 500 Hz/pixel; section thickness, 20 mm; field of view, 300 to 350 × 140 to 170 mm; image matrix, 110 × 256; and voxel size, 1.3 × 1.2 × 20.0 $mm^3$. For the MRI scan, each dog was anesthetized and a 16-gauge IV catheter was introduced into the right internal jugular vein. The dog was then fixed in a supine position and 3 mL of gadopentetate dimeglumine (Magnevist; Nihon Schering; Osaka, Japan) was administered as an IV bolus over 1 s. The contrast agent was administered immediately after the start of the dynamic imaging procedure. A total of 170 axial images were acquired to provide consecutive measurements over the 60-s scan time. The image immediately before the image showing any vascular enhancement was utilized as a mask image for subsequent image subtraction. For the imaging procedure, the signal intensity curves were measured from the right and left lung parenchymal areas (plotting area) separately. The mean signal intensity was calculated from the signal intensity curve during the 60-s scan time. The flow-volume ratio was calculated from the mean signal intensity of the left lung to the right lung, according to the following equation:

$$\text{Flow-volume ratio} = \frac{\text{mean signal intensity in left lung}}{\text{mean signal intensity in right lung}}$$

*Administration of FGF-2 Microspheres*

Human recombinant FGF-2 was supplied by Kaken Pharmaceutical Company, Tokyo, Japan. Gelatin was isolated from bovine bone collagen by an alkaline process using $CaOH_2$ (Nitta Gelatin Company; Osaka, Japan). FGF-2 microspheres with a diameter of approximately 10 μm were prepared as described previously by glutaraldehyde cross-linking of gelatin.[4,5] After washing with acetone (4°C), the microspheres were recovered by centrifugation. FGF-2 was radioiodinated and incorporated into the microspheres over a 1-h period before use. In the FGF + group, a total of 200 μg of FGF-2 was incorporated into each 4.0 mg of gelatin hydrogel microspheres. After performing a bronchoscopic examination, 4.0 mg of FGF-2 microspheres were suspended in 5 mL of saline solution and sprayed into the emphysematous left lung using a spray infusion catheter in 10 divided doses in a different area. The FGF − group were sprayed with 4.0 mg of gelatin hydrogel microspheres without FGF-2 using the same procedure into the left lung.

*Histologic Measurement*

Four weeks after treatment, the dogs in each group were euthanized by injection of pentobarbital sodium. The lung tissues and heart, along with the trachea, were resected *en bloc*. The heart and mediastinal tissues were removed, and the lungs with the attached trachea were weighed. The lungs were immediately inflated with 10% neutral buffered formalin solution via a tracheal cannula at a pressure of 25 cm $H_2O$ until the pleura became tense. The trachea was then ligated, and the lungs were fixed further by immersion in formalin solution for 48 h. The inflated lung volume was measured by the water replacement method, and the left and right lungs were measured separately.[7] Twenty 2 × 2×2-cm blocks were randomly cut from the whole area of the lung per animal. The blocks were then embedded in paraffin before being cut into 3-μm-thick sections and stained with hematoxylin-eosin. All the sections were used to measure mean linear intercept (Lm), a commonly used stereologic indicator of alveolar airspace enlargement in emphysema, which was calculated as described.[8] Sixty fields per animal at 40 × magnification were chosen at random to measure Lm.

*Statistical Analysis*

Data are expressed as mean (SD). Data were analyzed by analysis of variance using statistical software (StatView for Windows, version 5.0; SAS Institute; Cary, NC). Differences between groups were identified by a Scheffe test; p values $< 0.05$ were considered statistically significant.

## RESULTS

### *Distribution of FGF-2 Intratracheal Administration in the Rat*

Figure 1 shows a summary of the FGF-2 remaining after intratracheal administration in the rats. Radioactivity remaining after intratracheal administration decreased with time. In the FGF solution group, radioactivity count remaining at 24 h, 72 h, and 7 days was 35.4 ± 3.6, 5.4 ± 2.5, and 1.2 ± 0.17, respectively. In the FGF microsphere group, remaining levels of FGF-2 were significantly higher than in the FGF solution group ($p = 0.003$). Radioactivity remaining at 24 h, 72 h, and 7 days was 50.2 ± 10.5, 13.7 ± 1.6, and 2.9 ± 1.63, respectively. These results suggest that the controlled-release microsphere system increased the effectiveness of FGF-2.

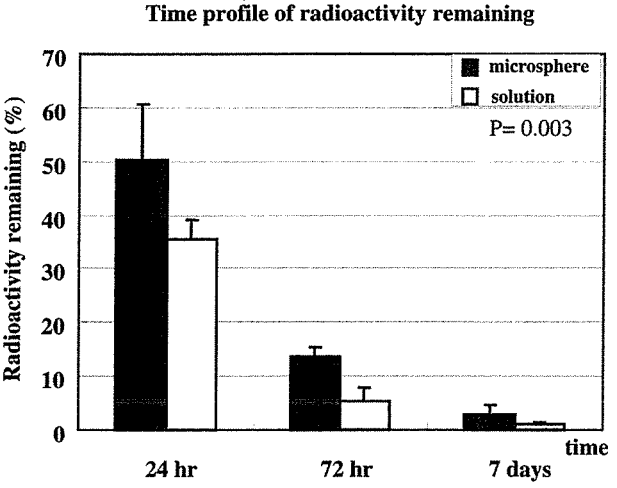


FIGURE 1. *In vivo* time profile of radioactivity remaining after intratracheal injection of gelatin microspheres incorporating $^{125}I$-labeled–FGF-2 (microsphere) or intratracheal injection of $^{125}I$-labeled–FGF-2 in aqueous solution (solution) into the rat trachea. In the FGF microsphere group, remaining levels of radioactivity were significantly higher than in the FGF solution group ($p < 0.01$). Data are presented as mean ± SD from nine rats per group at different time intervals: 24 h, 72 h, and 7 days.

### *Pulmonary Function Tests in the Canine Experiment*

Body weights did not differ between the FGF − group and the FGF + group: 11.4 ± 1.3 kg vs 11.8 ± 1.9 kg, respectively. There were no differences in body weight 4 weeks after elastase administration and 4 weeks after treatment (FGF − group, 11.6 ± 1.2 kg vs 11.5 ± 1.5 kg; FGF + group, 11.5 ± 2.1 kg vs 11.0 ± 2.3 kg). There was no evidence of serious side effects, including thrombocytopenia, anemia, or renal dysfunction, after FGF-2 administration.

Data for $PaO_2$ are shown in Figure 2, *top*, *A*. There were no differences in any parameters between the two groups at baseline and 4 weeks after elastase administration: FGF −, 95.5 ± 7.3 mm Hg vs 85.5 ± 3.0 mm Hg; FGF +, 92.8 ± 4.2 mm Hg vs 88.7 ± 3.4 mm Hg, respectively. Elastase-induced emphysema models had significantly lower $PaO_2$ values at 4 weeks after elastase administration than at the baseline ($p = 0.015$). Four weeks after treatment, $PaO_2$ in the FGF + group was significantly higher than in the FGF − group: 83.7 ± 4.6 mm Hg vs 95.3 ± 5.9 mm Hg ($p = 0.036$).

The intratracheal cavity was inflated at different

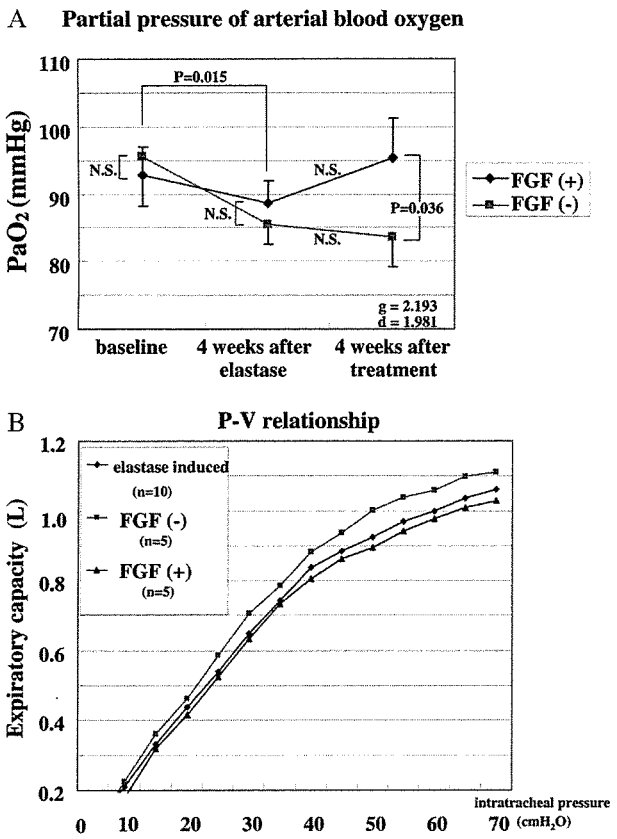


FIGURE 2. Results of pulmonary function tests in the FGF − group and the FGF + group. *Top, A*: Changes in $PaO_2$. Elastase-induced emphysema models had significantly lower $PaO_2$ values at 4 weeks after elastase administration than at baseline ($p = 0.015$). $PaO_2$ in the FGF + group was significantly higher than in the FGF − group at 4 weeks after treatment ($p = 0.036$). *Bottom, B*: The P/V relationship. The intratracheal cavity was inflated at different pressures (5 to 70 cm $H_2O$). Elastase-induced = elastase-induced emphysema models. The curve in the FGF − group was shifted upward to a greater extent than in the elastase-induced emphysema, whereas that in the FGF + group was shifted downward. N.S. = not significant.

pressures (5 to 70 cm $H_2O$). In the elastase-induced emphysema models, the P/V curve was shifted upward compared with the baseline. The curve in the FGF − group continued to shift upward, whereas that in the FGF + group shifted downward (Fig 2, *bottom, B*). The FGF + group appeared to exhibit better recovery than the FGF − group in terms of expiratory capacity with intratracheal pressure of 40 cm $H_2O$ (0.88 ± 0.20 L vs 0.79 ± 0.18 L), although the difference was not statistically significant ($p = 0.72$). These results suggested pulmonary functional recovery in the FGF + group.

### *Dynamic Contrast-Enhanced MRI*

MRI scans of pulmonary perfusion allowed the bolus of contrast agent to be followed through the superior vena cava, right atrium and ventricle, pulmonary arteries, lung parenchyma, pulmonary veins, left heart, and systemic arteries. At 5 s, the pulmonary arterial tree could be visualized beyond the segmental branches. A diffuse flash on the lung parenchyma was then observed, followed by a gradual increase in signal intensity over the next 20 s (Fig 3). In the elastase-induced emphysema models, the signal intensity was visually lower in the left lung. The left signal intensity was improved in the FGF + group. The difference between the left and right signals was maximal at 20 s. The signal intensity curves during the 60-s scan time are demonstrated in Figure 4. At the baseline, the levels of the signal intensity curves were the same in the right and left lungs. The signal intensity curve in the elastase-induced emphysema models declined in the left lung compared with the right (Fig 4, *top right, B*), and the signal intensity curve showed a sharply marked first-pass effect of enhancement with a significant lower-intensity peak on the pathologic side. The signal intensity curve in the FGF + group improved significantly in the left lung (Fig 4, *bottom right, C*). The flow-volume ratios at baseline were 0.99 ± 0.02 and 1.00 ± 0.04 in the FGF − group and the FGF + group, respectively (Fig 5). Four weeks after elastase administration, the flow-volume ratio was significantly lower than baseline: FGF − group, 0.70 ± 0.06; FGF + group, 0.69 ± 0.07. Four weeks after treatment, dynamic MRI revealed significant improvement in the FGF + group. The flow-volume

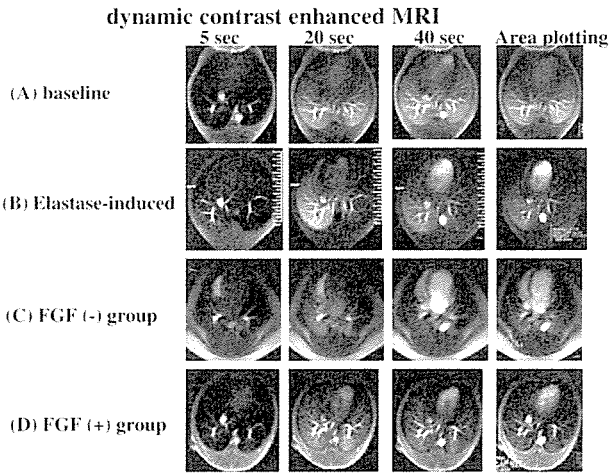


FIGURE 3. Dynamic contrast-enhanced MRI at baseline (*top row, A*), elastase-induced elastase-induced emphysema models (*upper center row, B*), the FGF − group (*lower center row, C*), and FGF + group (*bottom row, D*). At 5 s, the pulmonary arterial tree could be visualized beyond the segmental branches, followed by a gradual increase of signal intensity over the next 20 s. In the elastase-induced emphysema models, the signal intensity in the left lung was visually lower than that in the right lung. In the FGF + group, the signal intensity improved in the left lung, while the FGF − group showed no change.

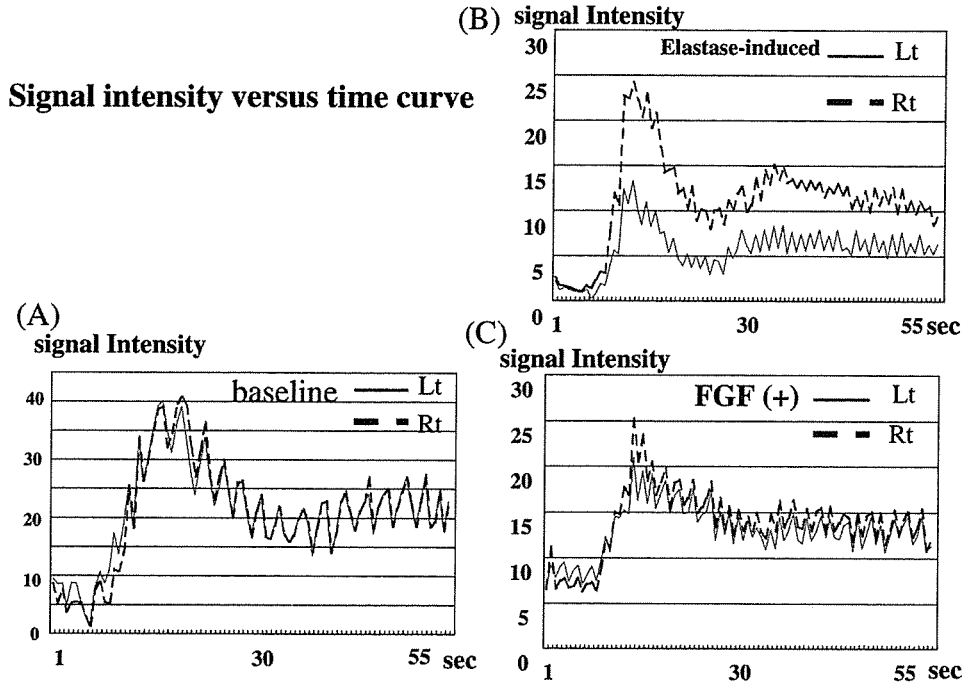


FIGURE 4. Signal intensity curves for the lung parenchyma (plotting area) after administration of gadopentetate dimeglumine during a 60-s scan time. *Left, A*: Baseline. The signal intensity curves for the left (Lt) and right (Rt) lungs were similar. *Top right, B*: Elastase-induced emphysema models. The signal intensity curve declined in the left lung compared with the right, and showed a sharply marked first-pass effect of enhancement with a significantly lower-intensity peak. *Bottom right, C*: FGF + group. Signal intensity curve was improved in the left lung.

ratio in the FGF + group was significantly improved after FGF-2 treatment, while the FGF − group score was the same as, or worse than, that in the dogs assessed before treatment: FGF −, 0.69 ± 0.05; FGF +, 0.88 ± 0.06 ($p = 0.0041$).

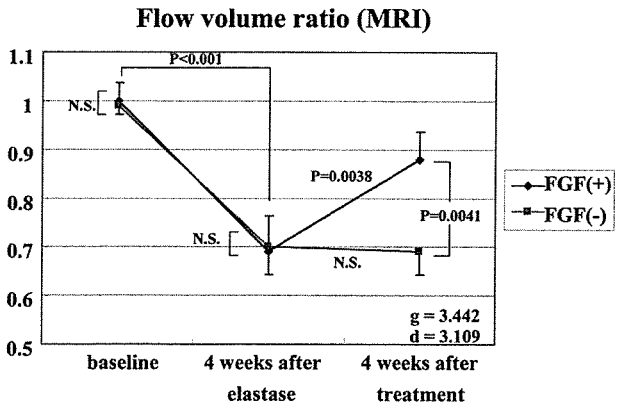


FIGURE 5. Flow-volume ratio determined by dynamic contrast-enhanced MRI. Four weeks after elastase administration, the flow-volume ratio was significantly lower than at baseline. The flow-volume ratio in the FGF + group was significantly improved after FGF-2 treatment, while the score for the FGF − group was the same as or worse than that for the dogs assessed before treatment. See Figure 2 legend for expansion of abbreviation.

*Lung Volumes and Histologic Findings*

A summary of the effects of FGF-2 on lung volume throughout the study period is presented in Figure 6. In the animals of the FGF − group, the left lung was overinflated compared with the control group. There were no changes in right lung volumes among the three groups. The left lung volume in the FGF + group was reduced compared to the FGF − group, although the difference was not statistically significant: control, 380.0 ± 82.9 $cm^3$; FGF −, 442.9 ± 50.4 $cm^3$; FGF +, 402.8 ± 71.8 $cm^3$. At autopsy, the tissue destruction caused by the elastase was associated with physiologic changes and a marked reduction in the surface area available for gas exchange (Fig 7). In the FGF + group, the mean size of alveoli was closer to control group than that of the FGF − group. There were no significant differences in right lung Lm levels among the three groups. Left lungs that had received elastase had a significantly increased Lm compared with the control group: control, 52.3 ± 2.8 μm; FGF −, 71.6 ± 4.0 μm; FGF +, 63.5 ± 3.2 μm. Lm levels in the control group and the FGF − group were significantly different ($p < 0.001$). The Lm value for the FGF + group appeared to indicate better recovery than in the FGF − group ($p = 0.02$).

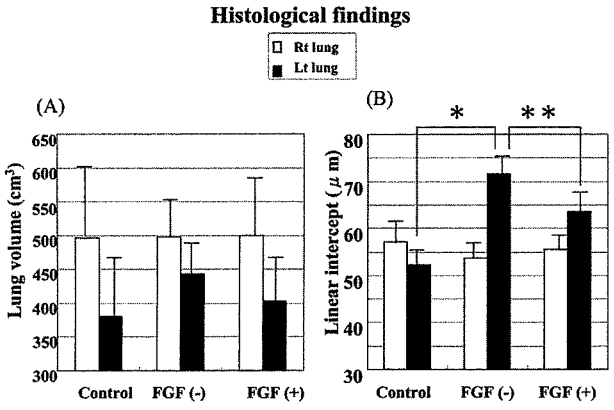


FIGURE 6. Histologic findings. *Left, A*: Lung volumes. *Right, B*: Linear intercept values. Left lung volumes in the FGF + group were reduced in comparison with the FGF − group. Left lungs that had received elastase showed significantly increased Lm values compared with those in the control group. *Lm levels in the control group and the FGF − group were significantly different from each other ($p < 0.001$). **The Lm value for the FGF + group appeared to indicate better recovery than in the FGF − group ($p = 0.02$). Rt lung = intact lung; Lt lung = treated lung.

## DISCUSSION

Growth factors and biological regulators have been evaluated experimentally with respect to their potential usefulness in promoting pulmonary parenchymal regeneration in emphysema.[9–11] Reports[11,14] have suggested that growth factors play an important role in fetal lung development in both rodents and humans. FGF is a member of the heparin-binding polypeptide family. It is widely distributed and has been identified in many tissues of neuroectodermal and mesodermal origin. FGF acts as an angiogenic molecule *in vitro*, while *in vivo* it stimulates smooth muscle cell growth, wound healing, and tissue repair.[12] FGF-2 is one of the most powerful angiogenic factors known and is indispensable for lung development and branching morphogenesis. Studies[13,14] of the expression of FGF-2 and receptors in the developing fetal rat lung have shown that FGF-2 immunoreactivity is localized to cells of the airway epithelium, basement membranes, and extracellular matrix. However, although these characteristics of FGF-2 indicate that it would be a potent promoter of pulmonary functional recovery in emphysema, its biological half-life is reported to be < 50 min, which is too short a time to maintain a sustained response. In addition, endothelial cells take almost 1 day to begin to respond to FGF-2 stimulation.[15,16] Hence, the simple administration of free FGF-2 results in few of the desired biological activities such as angiogenesis, branching morphogenesis, and pulmonary functional regeneration. In fact, some researchers[17] have reported that FGF-2 administration produces insufficient angiogenesis to induce revascularization and subsequent airway healing. We used controlled-release microspheres as vehicles for more effective induction of angiogenesis by FGF-2.

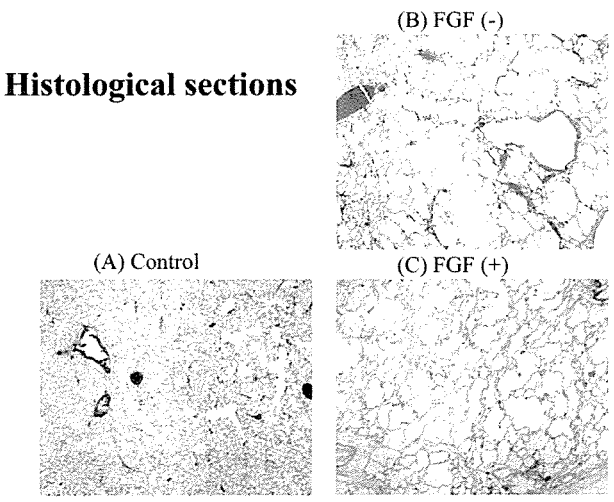


FIGURE 7. Representative photomicrographs of hematoxylin-eosin–stained sections (original × 40). *Left, A*: Control group; *top right, B*: FGF − group; and *bottom right, C*: FGF + group. The tissue destruction caused by the elastase was associated with physiologic changes and a marked reduction in the surface area. In the FGF + group, the mean size of alveoli was closer to the control group than that of the FGF − group.

When preparing microspheres, FGF-2 is incorporated into the hydrogel mainly as a result of physicochemical and electrical interactions between FGF-2 and the acidic gelatin, similar to the processes observed during hydrogen bonding and hydrophobic interactions.[4] Once incorporated, it is likely that the FGF-2 will be released from the gelatin hydrogel only when the hydrogel is enzymatically degraded to water-soluble gelatin fragments *in vivo*. A potential problem with this delivery system is therefore that FGF-2 release can only be controlled by changing the *in vivo* degradability of the gelatin hydrogels. This can be achieved by manipulating the water content of the hydrogels during their preparation.[4,5] We considered whether the microspheres could function as a drug delivery system in the airway and whether they had any unexpected side effects in the lung. In this *in vivo* study in rats, we compared the time profiles of the radioactivity remaining after intratracheal administration of $^{125}$I-labeled–FGF-2 either incorporated with an acidic gelatin hydrogel or as an aqueous solution. The gelatin hydrogel yielded a higher radioactivity count than the aqueous solution, thus confirming the effectiveness of the gel as a controlled-release mechanism. The controlled-release microspheres expanded the effects of FGF-2 and prolonged its biological half-life *in vivo*. There was no evidence of serious complications including infection, atelectasis, allergy, and hemorrhage after

gelatin hydrogels microspheres administration in this study. However, IV injection of hydrogels has a risk of vascular infarction. Therefore, gelatin microspheres cannot administer by the IV route.

Many groups have researched the lung parenchymal regeneration and alveolar septation for the chronic obstructive pulmonary diseases.[9,11,18] The mechanisms underlying regeneration and alveolar septation in the respiratory organs are still unclear, and it was not possible to determine whether FGF-2 treatment induced an increase in the number of alveoli or in alveolar septation. To date, we have found that FGF-2 treatment for COPD improves pulmonary function in the beagle dogs. The improvement in arterial oxygen gas data can be explained by the following: FGF-2 treatment led to a volume reduction in the affected lung and improvement of blood flow; subsequently, alveolar gas pressure also improved. Because oxygen uptake into the blood is dependent on the presence of a difference between the alveolar and capillary oxygen pressures, these improvements led to an improvement in the ventilation/perfusion shunt and in the gas exchange ability of the lung. In fact, little hypoxemia was observed after FGF-2 treatment, and the respiratory performance status of all dogs was improved, with no evidence of respiratory insufficiency.

There are some difficulties in attempting to achieve parenchymal regeneration and alveolar septation by the introduction of FGF-2 alone, because in the extracellular environment many growth factors and biological regulators interact with each other to produce parenchymal regeneration or alveolar septation.[13,19] It is difficult for tissue regeneration to occur in regions where blood flow is poor: pulmonary blood flow recovery is indispensable for lung regeneration and wound healing. Our present results indicate that the powerful angiogenic effect of FGF-2 induced both pulmonary revascularization and pulmonary vasodilation in the canine emphysema models, and suggest that this treatment may improve the symptoms of emphysema in humans. The magnitude of the physiologic improvement seen in response to FGF-2 treatment in this experimental model would be expected to benefit patients with severe emphysema to combine the intratracheal FGF-2 treatment and LVRS. We believe that intratracheal FGF-2 treatment has effective potential for emphysema, and that it will become one of the standard therapies for severe emphysema patients.

In conclusion, intratracheal administration of FGF-2 induced an increase in pulmonary blood flow in the damaged lung and volume reduction in the emphysematous lung. These changes led to an improvement in the ventilation/perfusion shunt and thus introduced the pulmonary functional recovery. The use of a controlled-release microsphere delivery system increased the effectiveness of FGF-2.

## References


1 National Emphysema Treatment Trial Research Group. A randomized trial comparing lung-volume-reduction surgery with medical therapy for severe emphysema. N Engl J Med 2003; 348:2059–2073

2 National Emphysema Treatment Trial Research Group. Cost effectiveness of lung-volume-reduction surgery for patients with severe emphysema. N Engl J Med 2003; 348:2092–2102

3 Doi M, Nakano K, Hiramoto T, et al. Significance of pulmonary artery pressure in emphysema patients with mild-to-moderate hypoxia. Respir Med 2003; 97:915–920

4 Tabata Y, Hijikata Y, Muniruzzaman MD, et al. Neovascularization effect of biodegradable gelatin microspheres incorporating basic fibroblast growth factor. J Biomater Sci Polymer Edn 1999; 10:79–94

5 Yamamoto M, Ikada Y, Tabata Y. Controlled release of growth factors based on biodegradation of gelatin hydrogel. J Biomater Sci Polymer Edn 2001; 12:77–88

6 Hatabu H, Tadamura E, Levin DL, et al. Quantitative assessment of pulmonary perfusion with dynamic contrast-enhanced MRI. Magn Reson Med 1999; 42:1033–1038

7 Scherle W. A simple method for volumetry of organs in quantitative stereology. Mikroskopie 1970; 26:S57–60

8 Gillooly M, Lamb D, Farrow ASJ. New automated technique for assessing emphysema on histological sections. J Clin Pathol 1991; 44:1007–1011

9 Massaro GD, Massaro D. Retinoic acid treatment abrogates elastase-induced pulmonary emphysema in rats. Nat Med 1997; 3:675–677

10 Krause DS, Theise ND, Collector MI, et al. Multi-organ, multi-lineage engraftment by a single bone marrow-derived stem cell. Cell 2001; 105:369–377

11 Selman M, Cisneros-Lira J, Gaxiola M, et al. Matrix metalloproteinases inhibition attenuates tobacco smoke-induced emphysema in guinea pigs. Chest 2003; 123:1633–1641

12 Bikfalvi A, Klein S, Pintucci G, et al. Biological roles of fibroblast growth factor-2. Endocr Rev 1997; 18:26–45

13 Chabut D, Fischer AM, Colliec-Jouault S, et al. Low molecular weight fucoidan and heparin enhance the basic fibroblast growth factor-induced tube formation of endothelial cells through heparan sulfate-dependent α6 overexpression. Mol Pharmacol 2003; 64:696–702

14 Ambalavanan N, Novak ZE. Peptide growth factors in tracheal aspirates of mechanically ventilated preterm neonates. Pediatr Res 2003; 53:240–244

15 Lazarous DF, Schinowitz M, Shou M, et al. Effects of chronic systemic administration of basic fibroblast growth factor on collateral development in the canine heart. Circulation 1995; 91:145–153

16 Schaper W, De Brabander M, Lewi P. DNA synthesis and mitoses in coronary collateral vessels of the dog. Circ Res 1971; 28:671–679

17 Behrend M, von Wasielewski R, Klempnauer J. Failure of airway healing in an ovine autotransplantation model that includes basic fibroblast growth factor. J Thorac Cardiovasc Surg 2002; 124:231–240

18 Lucey EC, Goldstein RH, Breuer R, et al. Retinoic acid does not affect alveolar septation in adult FVB mice with elastase-induced emphysema. Respiration 2003; 70:200–205

19 Pepper MS, Vassalli JD, Orci L, et al. Biphasic effect of transforming growth factor β1 on *in vitro* angiogenesis. Exp Cell Res 1993; 204:356–363

*Annals of Otology, Rhinology & Laryngology* 114(12):907-912.


# Destiny of Autologous Bone Marrow–Derived Stromal Cells Implanted in the Vocal Fold

Shin-ichi Kanemaru, MD, PhD; Tatsuo Nakamura, MD, PhD; Masaru Yamashita, MD; Akhmar Magrufov, MD; Tomoko Kita, PhD; Hisanobu Tamaki, MD; Yoshihiro Tamura, MD; Fuku-ichiro Iguchi, MD, PhD; Tae Soo Kim, MD; Masanao Kishimoto, MD; Koichi Omori, MD, PhD; Juichi Ito, MD, PhD

**Objectives:** The aim of this study was to investigate the destiny of implanted autologous bone marrow–derived stromal cells (BSCs) containing mesenchymal stem cells. We previously reported the successful regeneration of an injured vocal fold through implantation of BSCs in a canine model. However, the fate of the implanted BSCs was not examined. In this study, implanted BSCs were traced in order to determine the type of tissues resulting at the injected site of the vocal fold.

**Methods:** After harvest of bone marrow from the femurs of green fluorescent transgenic mice, adherent cells were cultured and selectively amplified. By means of a fluorescence-activated cell sorter, it was confirmed that some cells were strongly positive for mesenchymal stem cell markers, including CD29, CD44, CD49e, and Sca-1. These cells were then injected into the injured vocal fold of a nude rat. Immunohistologic examination of the resected vocal folds was performed 8 weeks after treatment.

**Results:** The implanted cells were alive in the host tissues and showed positive expression for keratin and desmin, markers for epithelial tissue and muscle, respectively. The implanted BSCs differentiated into more than one tissue type in vivo.

**Conclusions:** Cell-based tissue engineering using BSCs may improve the quality of the healing process in vocal fold injuries.

**Key Words:** bone marrow–derived stromal cells, cell-based tissue engineering, destiny of implanted cells, mesenchymal stem cells, regeneration, vocal fold.

## INTRODUCTION

Damaged tissues and organs do not naturally regenerate, because rapid growth of fibroblasts and/or epithelial cells generally robs them of space for regeneration. This natural course also holds true for the repair process of an injured vocal fold. After vocal fold injury, the vocal fold may atrophy or form scar tissue. This process causes permanent sequelae of dysphonia and dysphagia. The primary treatment for these disorders is augmentation. Although various materials have been used for vocal fold augmentation, the ideal substance for injection has not yet been found.[1-7] Treatment by injection of space-filling materials remains unsatisfactory.

Mesenchymal stem cells (MSCs) are pluripotent cells that have the potential to differentiate into chondrocytes, osteoblasts, adipocytes, fibroblasts, bone marrow stroma, and other tissues of mesenchymal origin.[8-10] The MSCs are capable not only of differentiation along specific lineages, but also of being recruited to tissues in need, and are widely distributed throughout the body. The bone marrow stroma is considered the source of a common pool of multipotent cells that gain access via the circulation to various damaged tissues in need of repair.[11] Bone marrow–derived stromal cells (BSCs) are easily accessible from bone marrow aspirates and are an enriched source of MSCs. There is great optimism that BSCs can be used to engineer an unlimited source of cells for repairing damaged tissues and organs.

We previously reported that injured vocal folds could be regenerated by implantation of selectively cultured autologous BSCs and atelocollagen in an experimental canine model (Figs 1 and 2).[12] Im-

From the Department of Otolaryngology–Head and Neck Surgery, Graduate School of Medicine (Kanemaru, Yamashita, Magrufov, Kita, Tamaki, Tamura, Iguchi, Kim, Kishimoto, Ito), and the Department of Bioartificial Organs, Institute for Frontier Medical Sciences (Nakamura), Kyoto University, Kyoto, and the Department of Otolaryngology, Fukushima Medical University School of Medicine, Fukushima (Omori), Japan.

Presented at the meeting of the American Broncho-Esophagological Association, Boca Raton, Florida, May 13-14, 2005.

**Correspondence:** Shin-ichi Kanemaru, MD, PhD, Dept of Otolaryngology–Head and Neck Surgery, Graduate School of Medicine, Kyoto University, 54 Kawahara-cho, Syogoinn, Sakyo-ku, Kyoto 606-8507, Kyoto, Japan.

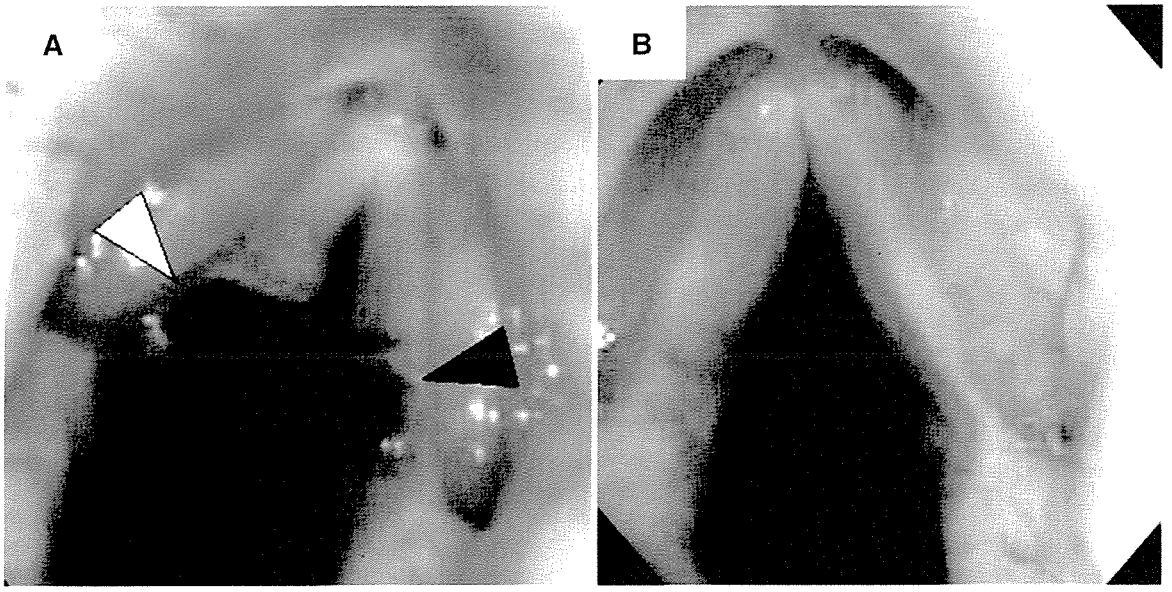


**Fig 1.** Morphological changes of vocal folds. **A)** Bilateral vocal folds were incised by electrocautery. Bone marrow–derived stromal cells (BSCs) with atelocollagen were implanted into left side of vocal fold (white arrowhead), and atelocollagen alone was injected into right side of vocal fold (black arrowhead). **B)** Morphological changes of injured vocal fold 2 months after treatment. Side with BSCs and atelocollagen implanted regenerated in almost normal shape, whereas atrophic changes occurred on side injected with atelocollagen alone.

planted BSCs undoubtedly play a key role in regeneration of the vocal fold; however, the fate of the implanted BSCs was not traced. Therefore, in this study, we focused on 2 issues: 1) characterization of cultured BSCs and 2) the types of host tissues derived from implanted BSCs.

## MATERIALS AND METHODS

*Animal Study.* In this study we used 4 GFP (green fluorescent protein) transgenic mice and 4 nude rats. Animal care, housing, and surgery were in accordance with the Guidelines of the Animal Experiment Committee of Kyoto University. The animals were anesthetized with ether and intramuscular administration of ketamine hydrochloride ($8.0 \times 10^{-4}$ mg/g; Sankyo Co, Tokyo, Japan) and xylazine hydrochloride ($5.0 \times 10^{-4}$ mg/g; Bayer, Tokyo). Antibiotics were administered for control of postsurgical infection. All animals underwent the same procedure pattern from the time of harvest of autologous bone marrow until

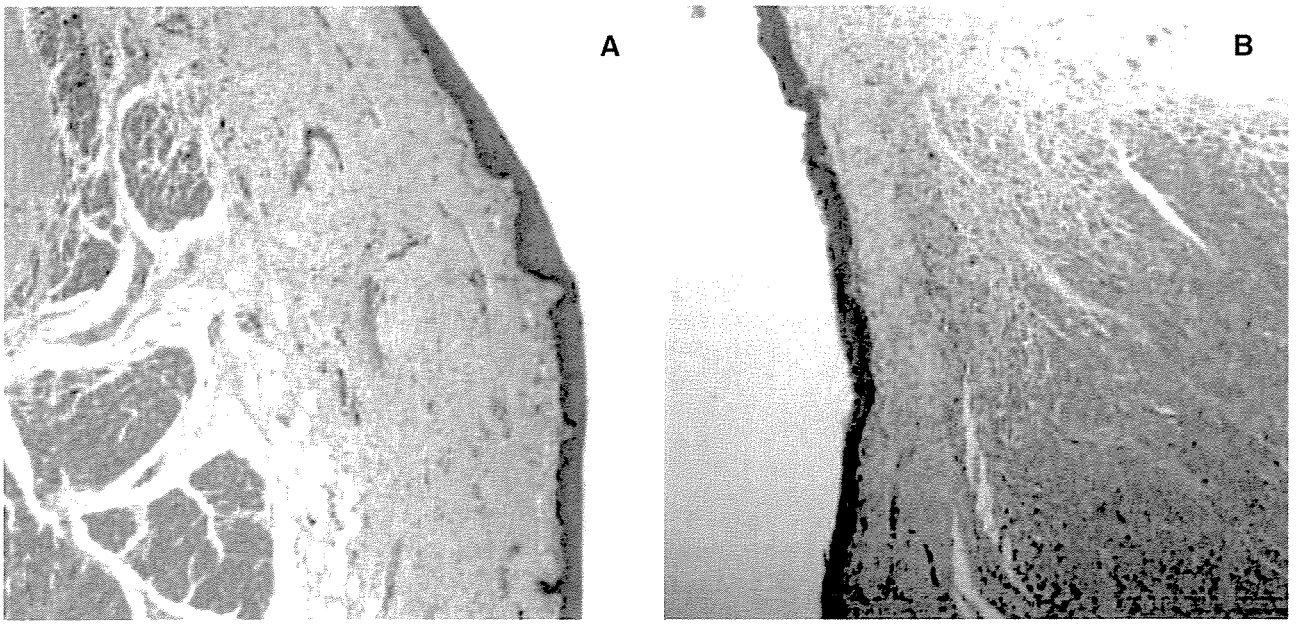


**Fig 2.** Vocal fold histology 2 months after treatment. **A)** BSCs with atelocollagen. Stratified structure of vocal fold is well regenerated. **B)** Atelocollagen alone. Scar formation between muscle and lamina propria is observed.

**Fig 3.** Fluorescent microscopic image of BSCs from GFP (green fluorescent protein) transgenic mouse 10 days after incubation.

they were painlessly sacrificed.

*Harvest and Culture of BSCs.* Under anesthesia, a GFP mouse was sacrificed and the bilateral femora were resected. By means of an injector with a 20-gauge needle, bone marrow was flushed from each femur and a single cell suspension was obtained. The bone marrow cells were placed in a 10-cm-diameter Petri dish with 15 mL of Dulbecco's modified Eagle's medium (DMEM) containing 10% fetal bovine serum and an antibiotic-antimycotic mixture (Gibco, Invitrogen Co, Carlsbad, California). The cells were incubated in 5% carbon dioxide at 37°C (MCO-17AIC carbon dioxide incubator, Sanyo Co, Osaka, Japan) for 48 hours in order to allow the BSCs time to adhere to the bottom of the dish. On day 3, the culture medium containing undesired floating contaminants, including hematopoietic cells and waste products, was removed to leave only adherent cells on the bottom of the dish (Fig 3). Fresh medium was then added and exchanged every 3 days. To amplify the number of BSCs, we continuously cultured cells for 14 days.

After 2 weeks, confluent growth of the cultured cells was confirmed microscopically (Olympus, IX70; Olympus Co, Tokyo) and the cells were detached from the bottom of the dish by addition of 2 mL of trypsin with 0.25% ethylenediaminetetraacetic acid (EDTA; Invitrogen Co). Approximately $2 \times 10^6$ to $6 \times 10^6$ cells were recovered from each plate. After neutralization of the trypsin solution, thorough washing of the cells with DMEM, and concentration by centrifugation at 3,500 rpm for 3 minutes (LX-120 centrifuge; Tomy Co, Tokyo), the cells were ready for injection or fluorescence-activated cell sorter (FACS) analysis.

*Fluorescence-Activated Cell Sorter Analysis.* The BSCs were cultured in control medium for 14 days before FACS analysis. The cells were stained with antibodies to Sca-1 (Ly-6A/E; eBioscience, San Diego, California), CD29 (Santa Cruz Biotechnology, Inc, Santa Cruz, California), CD34, CD44, CD45, CD49e, and 7-AAD (all from Becton Dickinson Biosciences, San Jose, California).

The MSCs were detached with trypsin-EDTA and counted. Approximately $1 \times 10^5$ cells were divided into aliquots in 5-mL centrifuge tubes and pelleted by centrifugation for 3 minutes at 400*g*. The cells were resuspended in 0.2 mL phosphate-buffered saline solution containing 1 mmol/L EDTA and 0.1% fetal bovine serum along with antibody combinations and incubated at room temperature for 20 minutes. Excess antibody was removed by washing. The cells were run on an FACS Calibur cytometer (Becton Dickinson and Company, Franklin Lakes, New Jer-

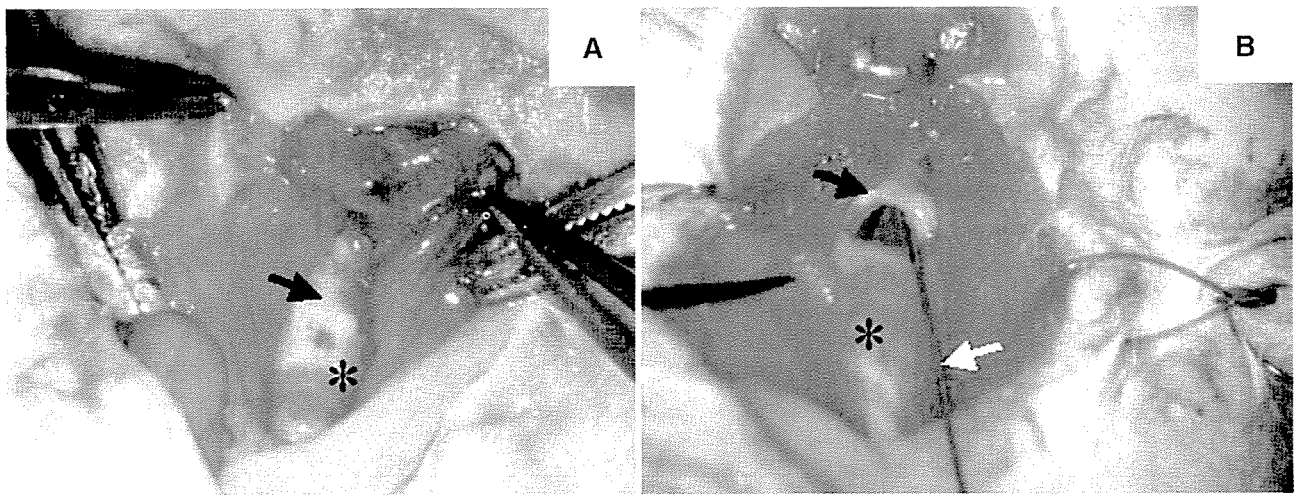


**Fig 4.** Surgical procedure. Black arrows — cricoid cartilage; asterisks — trachea. **A)** Vocal fold and surrounding tissues of nude rat are injured with 32-gauge needle through incision made at lower border of cricoid cartilage. **B)** BSCs from GFP mouse ($1 \times 10^5$ to $3 \times 10^5$) are injected into damaged areas. White arrow — 32-gauge needle.

SURFACE ANTIGEN EXPRESSION OF BONE MARROW–DERIVED STROMAL CELLS

| *Surface Antigen* | *Percent Positive* |
|---|---|
| CD29 (integrin β1) | >75 |
| CD34 | 2-20 |
| CD44 | >75 |
| CD45 | 2-20 |
| CD49e (integrin α5β1) | 20-75 |
| Sca-1 | >75 |

sey) and analyzed with Cell Quest software from a minimum of $1 \times 10^4$ collected events.

*Surgical Procedures.* Under anesthesia, a vertical skin incision was made on the neck of a nude rat and the larynx was exposed (Fig 4A). A half incision was made at the lower border of the cricoid cartilage, and the vocal fold and surrounding tissues were injured with a 32-gauge needle (Fig 4B). Fourteen-day cultured BSCs from a GFP mouse ($1 \times 10^5$ to $3 \times 10^5$) were injected into the damaged areas with an injector with a 32-gauge needle. The incision was sutured with 6-0 Maxon (Ladary Japan, Tokyo). All surgical procedures were performed under a surgical microscope (Olympus OME KA-1; Olympus Co), and sterile techniques were used throughout the procedures. After surgery, all rats were given injectable antibiotics.

*Histology.* The nude rats were painlessly sacrificed 8 weeks after injury and BSC implantation. Immediately after sacrifice, the larynx and the upper part of the trachea were resected and fixed in 4% paraformaldehyde. Histologic examination consisted of an immunofluorescent technique using monoclonal antibodies (Cosmo Bio Co, Ltd, Tokyo) to keratin (epithelial cells) and desmin (muscle).

## RESULTS

*Phenotypic Characterization of BSC Populations.* The expression of surface antigens on BSCs cultured for 14 days is shown in the Table. The BSCs expressed CD29, CD44, CD49e, and Sca-1, all markers for murine MSCs.[13] In addition, expression of

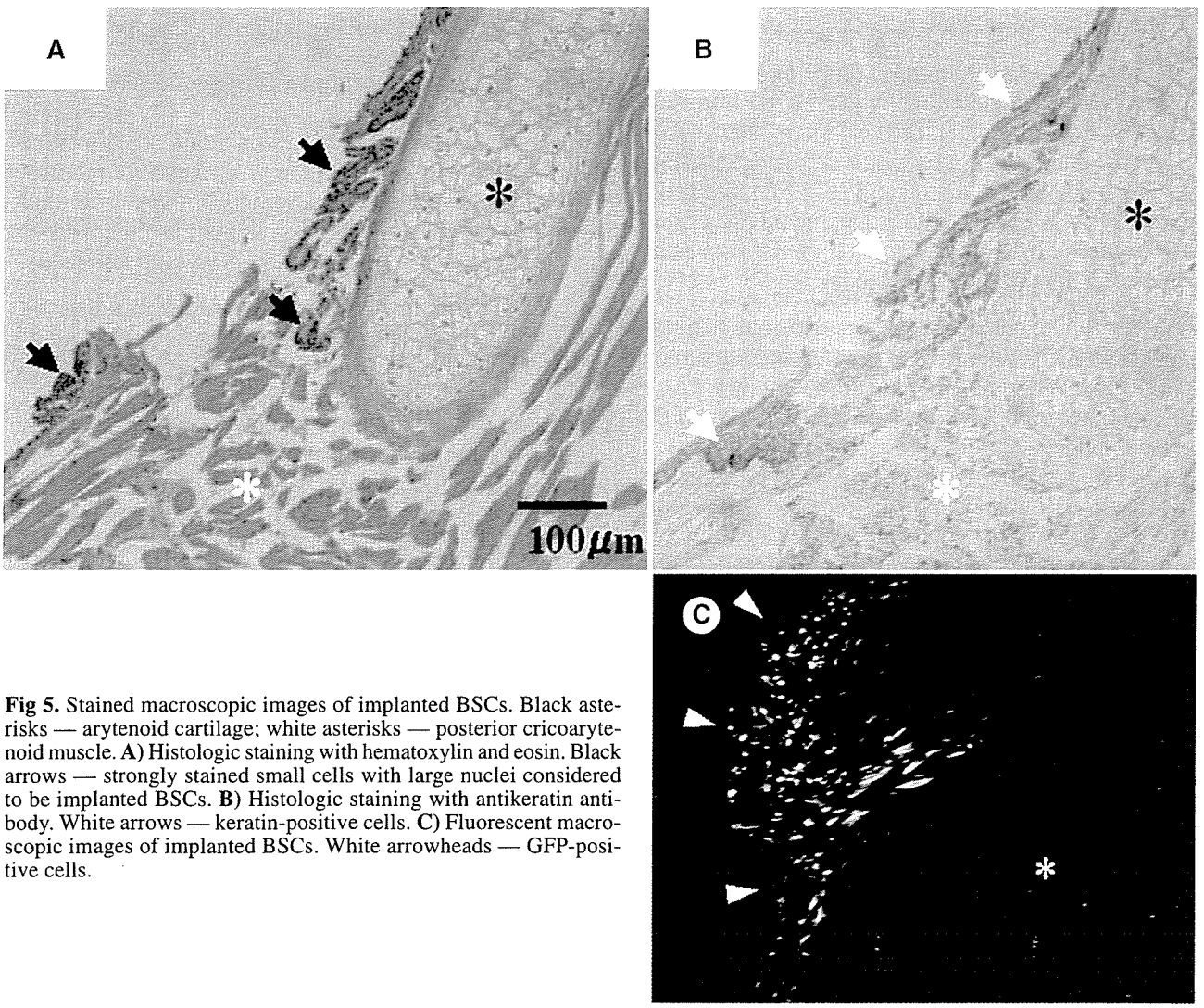


**Fig 5.** Stained macroscopic images of implanted BSCs. Black asterisks — arytenoid cartilage; white asterisks — posterior cricoarytenoid muscle. **A)** Histologic staining with hematoxylin and eosin. Black arrows — strongly stained small cells with large nuclei considered to be implanted BSCs. **B)** Histologic staining with antikeratin antibody. White arrows — keratin-positive cells. **C)** Fluorescent macroscopic images of implanted BSCs. White arrowheads — GFP-positive cells.

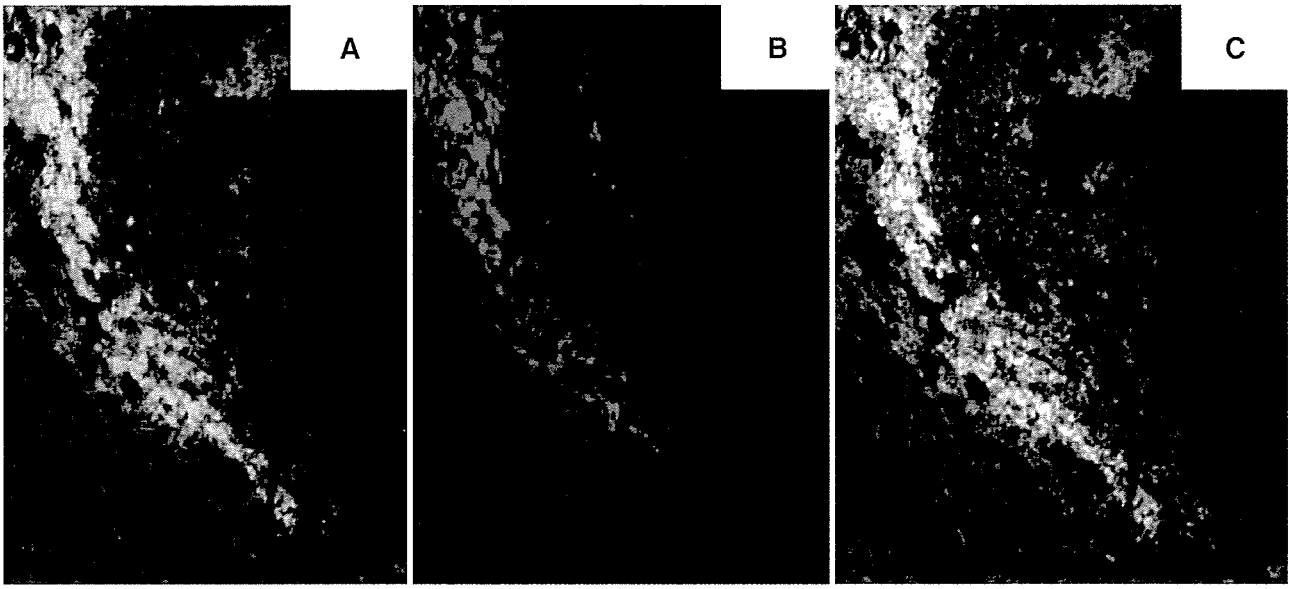


**Fig 6.** Fluorescent macroscopic images of implanted BSCs. **A)** GFP-positive cells. **B)** Desmin-positive cells. **C)** Composite of both images.

the hematopoietic lineage markers CD34 and CD45 was also observed in these cells.

*Differentiation of Implanted BSCs in Nude Rats.* All nude rats remained healthy during the observation period. In the lumen of the larynx, there were strongly stained small cells with a large nucleus (Fig 5A) that also stained for keratin (Fig 5B) and GFP (Fig 5C). These results demonstrate that BSCs from a GFP mouse differentiated into epithelial tissues in the peripheral regions of the vocal fold.

Cells positive for desmin were also found in the laryngeal lumen and mirrored the staining pattern of GFP (Fig 6). When the GFP and desmin staining patterns were merged, both desmin-positive and GFP-positive cells were observed, indicating that implanted BSCs differentiated into muscle cells. On the other hand, desmin-positive and GFP-negative cells were also observed in the same area, indicating the original host muscle cells. These results demonstrate that implanted BSCs differentiated into muscle cells in and around the original host muscle.

## DISCUSSION

Stem cells are defined as a cell population that possesses self-renewal capacity and multilineage potential. There are many kinds of stem cells, including embryonic stem cells, MSCs, and neural stem cells. Embryonic stem cells have the largest potential and are the ideal source for therapeutic applications.[14,15] However, because embryonic stem cells are derived from the blastocyst inner cell mass, the issue of rejection is a concern, as are the multiple ethical and social concerns surrounding the use of embryonic stem cells. Thus, MSCs and BSCs have been proposed as an alternative source of stem cells.[11] The MSCs are described as multipotent, because of their ability to differentiate into a variety of different cells and tissue lineages. The BSCs are easily accessible via bone marrow aspirate and contain a rich source of MSCs that are easy to obtain and culture in vitro. Because these cells are autologous, there is neither rejection by the immune system nor the ethical problems encountered in the use of embryonic stem cells.

Although many studies have used MSCs derived from bone marrow, the cells are poorly characterized.[11,13] In this study, murine BSCs that were cultured for 14 days before implantation contained cells positive for the MSC surface markers CD29, CD44, CD49e, and Sca-1. In addition, expression of the hematopoietic lineage markers CD34 and CD45 was also observed in these cells, indicating that BSCs grown in this manner are composed of at least 2 lineage cell groups.

The vocal fold is composed mainly of 3 layers: the epithelial layer, the lamina propria, and the muscular layer. The lamina propria has the most important role in mucosal vibration. Although the atrophy and scarring that cause permanent dysphonia are observed primarily in this layer, they also occur in the other 2 layers. Therefore, for recovery of good phonation, it is insufficient to regenerate a single layer alone. This vocal fold tissue complexity makes treatment difficult.

Many treatments for vocal fold insufficiency have been reported.[1-7] The majority of these treatments include augmentation of the damaged vocal fold.

Various materials have been used for vocal fold augmentation, such as collagen, Teflon,[3] hyaluronic acid,[6] autologous fat,[4,5] and autogenous fascia.[7] However, simply injecting space-filling materials does not prevent vocal fold deformation. According to tissue engineering doctrine, a scaffold should be designed to encourage regeneration by cells residing at the site of transplantation. Collagen is a widely distributed extracellular matrix and a functionally essential component of vocal fold structure.[16,17] In our previous study, BSCs and atelocollagen were used as cells and as a scaffold, respectively. Although collagen is thought to be an ideal scaffold, it does not induce cellular regeneration in the damaged vocal fold; therefore, the vocal fold is unable to regenerate by transplantation of a scaffold alone. The success of regeneration depends on appropriate replenishment of cognate stem cells at the damaged site. From this viewpoint, BSC-based tissue engineering is essential for regeneration of the vocal fold.

Implanted BSCs undoubtedly play an important role in tissue regeneration. There is a possibility that BSCs directly differentiate into many kinds of tissues in vivo and/or stimulate host organs into regeneration. This study demonstrated that a portion of implanted BSCs could differentiate into 2 different tissue lineages — epithelial cells and muscle cells — in a damaged vocal fold and peripheral tissues. However, it remains to be determined whether implanted BSCs can differentiate into other tissues to work as a trigger for regeneration. Further studies are needed to determine the use of BSCs for clinical treatment.

## CONCLUSIONS

In this study, we demonstrated that implanted BSCs were composed of at least 2 different lineage cell groups containing MSCs, and that they differentiated into 2 different tissue lineages in vivo: epithelial cells and muscle cells. It is possible that BSCs can be engineered as an unlimited source of cells to repair damaged complex tissues and organs such as the vocal fold.

**Acknowledgments:** The authors thank Satoshi Fujita for advice on fluorescence-activated cell sorter analysis and Dr Yoshinobu Toda for his histology expertise.

## REFERENCES

1. Ford CN, Martin DW, Warner TF. Injectable collagen in laryngeal rehabilitation. Laryngoscope 1984;94:513-8.

2. Ford CN, Staskowski PA, Bless DM. Autologous collagen vocal fold injection: a preliminary clinical study. Laryngoscope 1995;105:944-8.

3. Trapp TK, Berke GS, Bell TS, Hanson DG, Ward PH. Effect of vocal fold augmentation on laryngeal vibration in simulated recurrent laryngeal nerve paralysis: a study of Teflon and Phonogel. Ann Otol Rhinol Laryngol 1989;98:220-7.

4. Mikaelian DO, Lowry LD, Sataloff RT. Lipoinjection for unilateral vocal cord paralysis. Laryngoscope 1991;101:465-8.

5. Brandenburg JH, Unger JM, Koschkee D. Vocal cord injection with autogenous fat: a long-term magnetic resonance imaging evaluation. Laryngoscope 1996;106:174-80.

6. Hallen L, Dahlqvist A, Laurent C. Dextranomeres in hyaluronan (DiHA): a promising substance in treating vocal fold insufficiency. Laryngoscope 1998;108:393-7.

7. Rodgers BJ, Abdul-Karim FW, Strauss M. Histological study of injected autologous fascia in the paralyzed canine vocal fold. Laryngoscope 2000;110:2012-5.

8. Pittenger MF, Mackay AM, Beck SC, et al. Multilineage potential of adult human mesenchymal stem cells. Science 1999; 284:143-7.

9. Deans RJ, Moseley AB. Mesenchymal stem cells: biology and potential clinical uses. Exp Hematol 2000;28:875-84.

10. Woodbury D, Schwarz EJ, Prockop DJ, Black IB. Adult rat and human bone marrow stromal cells differentiate into neurons. J Neurosci Res 2000;61:364-70.

11. Tuan S, Boland G, Tuli R. Adult mesenchymal stem cells and cell-based tissue engineering. Arthritis Res Ther 2003;5:32-45.

12. Kanemaru S, Nakamura T, Omori K, et al. Regeneration of the vocal fold using autologous mesenchymal stem cells. Ann Otol Rhinol Laryngol 2003;112:915-20.

13. Meirelles Lda S, Nardi NB. Murine marrow-derived mesenchymal stem cell: isolation, in vitro expansion, and characterization. Br J Haematol 2003;123:702-11.

14. Daley GQ, Goodell MA, Snyder EY. Realistic prospects for stem cell therapeutics. Hematology (Am Soc Hematol Educ Program) 2003:398-418.

15. Rippon HJ, Bishop AE. Embryonic stem cells. Cell Prolif 2004;37:23-34.

16. Sato K, Hirano M, Nakashima T. Fine structure of the human newborn and infant vocal fold mucosae. Ann Otol Rhinol Laryngol 2001;110:417-24.

17. Ishii K, Zhai WG, Akita M, Hirose H. Ultrastructure of the lamina propria of the human vocal fold. Acta Otolaryngol (Stockh) 1996;116:778-82.

喉頭 17：84～88, 2005.　シンポジウムII：喉頭・気管領域のトランスレーショナルリサーチ

# 気道の再生

多田靖宏・野本幸男・鈴木輝久・大森孝一

# Regenerative Medicine of the Airway Tract

Yasuhiro Tada, Yukio Nomoto, Teruhisa Suzuki and Koichi Omori

Airway reconstruction after resection of malignancies or stenotic inflammatory lesions after traumatic injury is one of the most difficult procedures. To provide functional regeneration of the airway, we used *in situ* Tissue Engineering technique. As the tissue scaffold, Marlex mesh reinforced with polypropylene rings covered by a collagen sponge was developed. This scaffold material was implanted in animal models. After the safety and the utility were confirmed in the animal studies, the current regenerative technique was applied in human clinical cases with good results. However the growth speed of the tracheal epithelium over the artificial material was slow. To solve this problem, we tried to develop a hybrid material with which to cover the epithelium of the trachea. In this paper we report the basic research results of tissue engineering for the airway tract to date and of its clinical application. Furthermore, we report our current development of the hybrid artificial material.

**Key words**：再生，気道，気管上皮細胞

## 1．はじめに

癌や外傷などで気道の組織が侵された場合，これを切除した後に機能障害なく再建することは難しい．本研究の目的は気道臓器の機能的再生をはかり，気道病変切除後の呼吸，嚥下，発声，構音の機能障害を回避し，Quality of Life の向上を実現することにある．気道の再生アプローチとして気管・気管支・声帯に対する報告はすでになされているが[1, 2]，現在われわれは細胞や組織，動物を扱う基礎研究の成果を臨床に橋渡しするトランスレーショナルリサーチにより，有効かつ安全な喉頭・気管の再生治療の確立を目指している．

本稿では，現在までの基礎研究の成果，および臨床応用の結果を呈示し，さらに問題点を解決するために基礎研究へフィードバックし，現在われわれが取り組んでいるハイブリッド人工材料について述べる．

## 2．人工気管の作製と動物実験

臓器再生の三要素として，足場，適切な細胞，環境調節因子が必要であり，その場所に血流が供給されることで臓器再生が促されるとされている[1~3]．Nakamura ら[4]は，体内の再生を目的とする臓器の場所で組織を再生させる in situ Tissue Engineering という概念に基づき研究をすすめてきた．1995年 Teramachi ら[5]は気管欠損に対する再建材料として，管状の枠組みを保持するためポリプロピレン性のメッシュを管状にし，さらに同質の材料でリング状に補強し，組織再生の足場として周囲にコラーゲンスポンジを付加した組織再生型人工気管を開発した．ポリプロピレンメッシュは特定医療保険材料として従来から臨床応用されている材料であり，コラーゲンスポンジは医療用のブタ皮膚由来のI型およびIII型コラーゲンを用いている．また，実際にイヌに移植した後，再生気管に対し圧縮試験を行い正常気管と同程度の強度を保つことを確認している．

また，Nakamura ら[4]は動物実験として，全身麻酔下でビーグル犬において約4 cm の気管管状切除モデルを作製したうえで人工材料を移植し，その1年後の摘出標本にて上皮化と線毛上皮の再生を確認した．また，内視鏡による最長5年の観察にて再生気管に問題がなかったと報告している．

## 3．臨床応用

以上の基礎実験をもとに，2002年京都大学倫理委員会で「喉頭・気管の再生治療」の承認を得て現在まで2例の臨床応用を行っており最長2年1ヶ月の観察で経過良好である[6]．本学においても2003年に倫理委員会の承認を得て現在まで2例の臨床応用を行っている．本学で行った第1例目は，喉頭気管狭窄例で，77歳，男性．主訴は呼吸困難．以前の気管切開孔に対する閉鎖術の後，感染により声門下

福島県立医科大学医学部耳鼻咽喉科学講座
Department of Otolaryngology, Fukushima Medical University School of Medicine

から頸部気管に肉芽の増生を認め気道内腔の径が約5mmに狭小化していた．

手術は，局所麻酔下に再度気管切開術を行い，その後全身麻酔下に不良肉芽除去を行った．この際，輪状軟骨，甲状軟骨下縁も瘢痕組織となっておりこれらの軟骨の一部も含めて切除した．その後，13×6mmの欠損部に対し，人工材料をトリミングして30×15mmにしたものに自己の血液を湿潤させ，これで被覆して縫合した（図1）．

術後の内視鏡所見で，人工材料内腔面に対し術後3日，2週間では上皮化は不十分で，術後2ヶ月でようやく上皮化を確認できた（図2）．術後3ヶ月を経過した現在も再狭窄はきたしていない．この症例からは，ヒト喉頭気管においては人工材料上の上皮化に約2ヶ月間を要すると考えた．

### 4．基礎研究へのフィードバック：ハイブリッド人工材料の作製と移植

人工材料を用いた再建の利点として，低侵襲であり症例によっては気管切開が不要となり，また2次手術が不要となる可能性が挙げられる．一方，臨床応用の結果よりその問題点として，上皮化の速度が遅いことが挙げられる．そこで，人工材料の表面に気管上皮細胞層を形成してハイブリッド材料を作製することにより，上皮化を促進することが可能となるのかについて，ラットの気管欠損モデルを作製し，これにハイブリッド材料の移植実験を行った．

1）気管上皮細胞の採取・培養

SD系ラットの気管を摘出し，4℃，24～48時間プロテアーゼ処理を行い，気管上皮細胞を採取する．洗浄後，Penicillin G®，Streptomycin®，Amphotericin B®，及

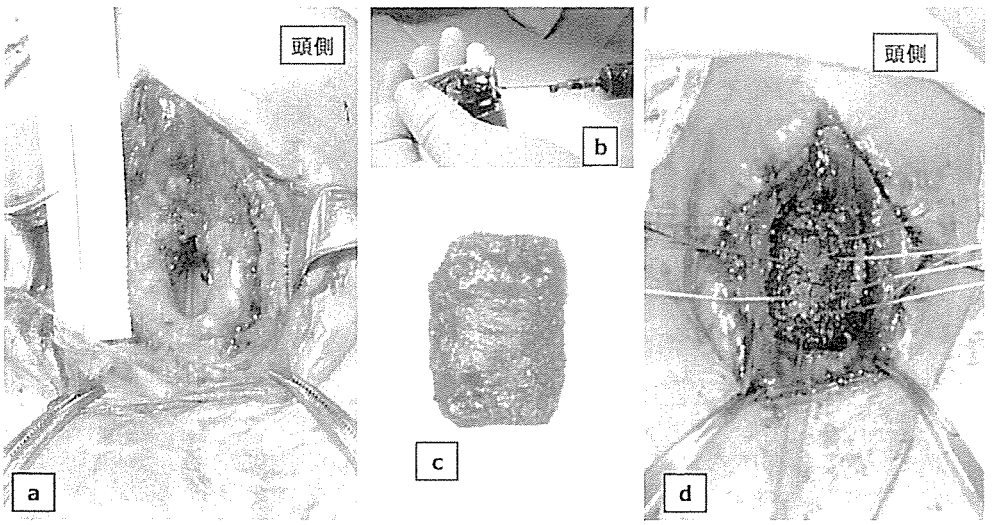


図1　臨床応用：喉頭気管狭窄例
a．欠損部　13×6mm
b．人工材料に自己の末梢血を湿潤
c．人工材料　30×15mm
d．被覆後に縫合

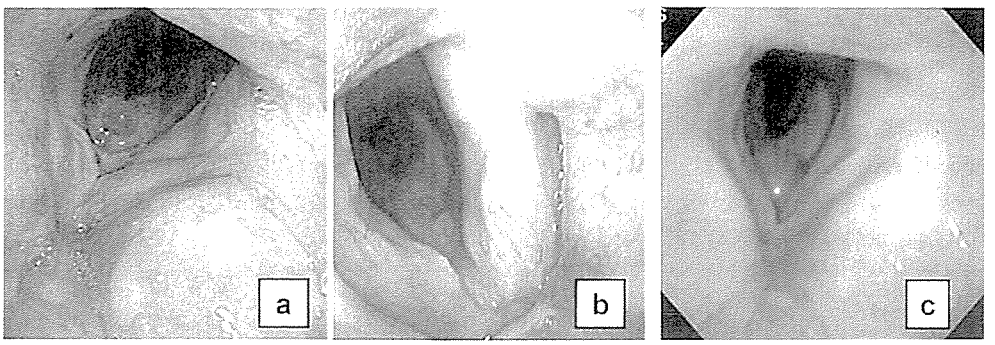


図2　内視鏡所見
a．術後3日目：上皮化認めず
b．術後2週間：上皮化不十分
c．術後2ヶ月：上皮化認める

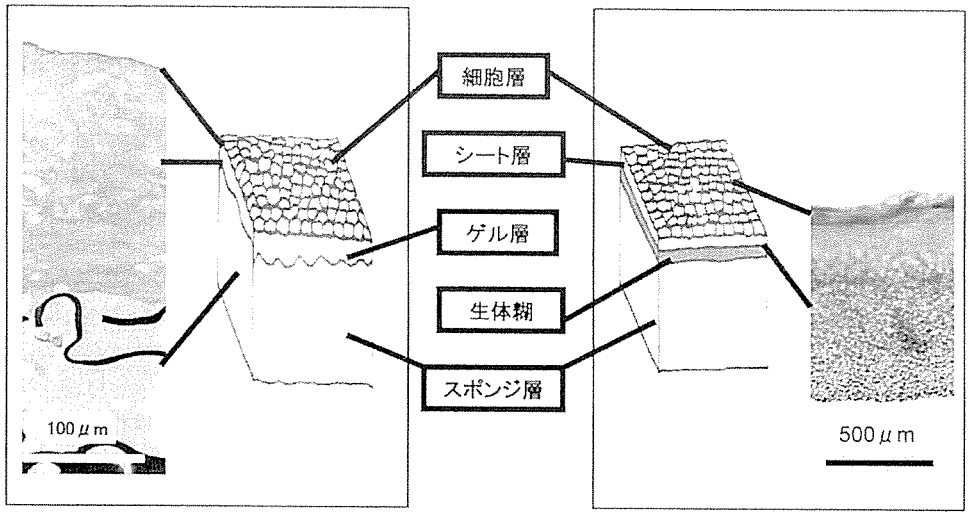


図3　ハイブリット型人工材料のHE染色と構造模式図
Type A：表面はやや不整
Type B：表面は平滑

び15% Fetal bovine serumを添加したDMEM培地で細胞懸濁液を作製し，継代培養法を確立した．

2）ハイブリット型人工材料の作製

培養した細胞を用いてハイブリット型の人工材料を2種類作製した．Type Aはすでに臨床応用されているコラーゲンスポンジ上に豚腱由来のⅠ－A型コラーゲンに再構成用緩衝液を作用させ生じたコラーゲンゲルを重層化し，次いで培養皿の底に留置して細胞懸濁液を満たし，表面に気管細胞層を形成させたものである．Type Bは，組織培養用コラーゲン膜（cellgen®）を培養皿に留置し，細胞懸濁液を満たして表面に気管細胞層を形成させ，後にコラーゲンスポンジと生体糊で接着させたものである．それぞれの構造的特徴はType Aの表面はやや不整であり，それに対しType Bの表面は平滑なものである．それぞれのハイブリット型人工材料についてパラフィン切片を作製し，H-E染色にて観察したところ人工材料の表面に気管上皮細胞層の形成を確認できた（図3）．免疫染色での観察ではType Aにて基底膜の指標となるcytokeratin14と，上皮細胞の指標となるcytokeratin18で培養上皮細胞での発現を認め，タイトジャンクションの指標となるoccludinにおいても発現が認められた．Type Bにおいてはoccludinの培養上皮細胞での発現を認め，膜輸送タンパクの指標となるNa-K-ATPaseと，増殖能の指標となるPCNAの培養上皮細胞での発現を認めた（図4）．これらの結果より作製した人工材料上の気管上皮細胞層は上皮の性質を有すると考えられた．

3）動物実験

作製したハイブリット型人工材料Type AとType Bの上皮細胞をin vivoにて移植した際に上皮細胞が生着するかどうかを，ラットの気管欠損モデルを作製し，これらを移植して評価した．

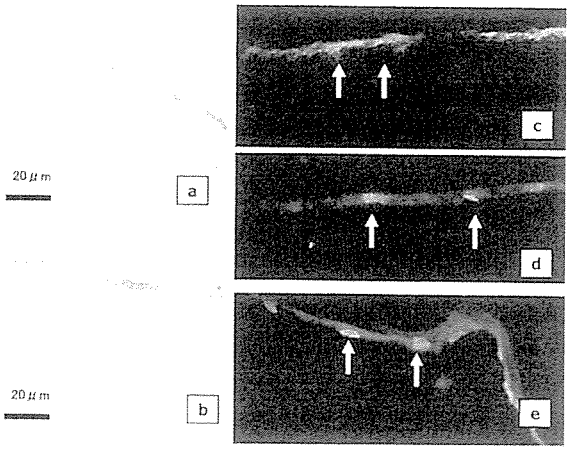


図4　免疫染色：気管上皮細胞にて陽性
a．cytokeratin14：(矢印)
b．cytokeratin18：(矢印)
c．occludin：(矢印)
d．Na-K-ATPase：(矢印)
e．PCNA：(矢印)

ラットの気管を露出し，電気メスを用いて約4×2mmの欠損を作り，人工材料Aを被覆したモデルと，人工材料Bを被覆したモデルを作製した．人工材料上の気管上皮細胞には9W齢SD系GFP遺伝子改変導入ラットより採取し培養した細胞を用いた．観察期間はそれぞれ3日・7日・30日とした．

Type A移植モデルのHE染色にて術後3日では欠損部に一致して人工材料を認め，その表面に上皮層の形成を認めた．免疫染色にて創部にGFP陽性細胞層を認めており（図5a，c），これと同様の所見が術後7日でも確認されたが，術後30日では確認できなかった．

Type B移植モデルのHE染色にて術後3日では欠損部